UNCLASSIFIED

AD 457058

DEFENSE DOCUMENTATION CENTER

FOR

SCIENTIFIC AND TECHNICAL INFORMATION

CAMERON STATION ALEXANDRIA, VIRGINIA

UNCLASSIFIED

NOTICE: When government or other drawings, specifications or other data are used for any purpose other than in connection with a definitely related government procurement operation, the U. S. Government thereby incurs no responsibility, nor any obligation whatsoever; and the fact that the Government may have formulated, furnished, or in any way supplied the said drawings, specifications, or other data is not to be regarded by implication or otherwise as in any manner licensing the holder or any other person or corporation, or conveying any rights or permission to manufacture, use or sell any patented invention that may in any way be related thereto.

ATALOGED BY: DDC
AD No. 459058

Final Report

PRESSURE TRANSDUCER FOR MEASURING SHOCK WAVE PROFILES
PHASE IX: ADDITIONAL GAGE DEVELOPMENT

Prepared for:

DEFENSE ATOMIC SUPPORT AGENCY
WASHINGTON, D.C. 20301

CONTRACT NO. DA-49-146-XZ-096

459058

DASA 1414-1

November 30, 1964

Final Report

PRESSURE TRANSDUCER FOR MEASURING SHOCK WAVE PROFILES PHASE IX: ADDITIONAL GAGE DEVELOPMENT

Prepared for:

DEFENSE ATOMIC SUPPORT AGENCY
WASHINGTON, D.C. 20301

CONTRACT NO. DA-49-146-XZ-096

By: D. D. KEOUGH
POULTER RESEARCH LABORATORIES

SRI Project GSU-3713

Work on this contract was initiated under sponsorship of the Advanced Research Projects Agency as part of the VELA UNIFORM Point-Source Program and has been continued by the Defense Atomic Support Agency under Subtask Number 13.118.

Approved: D. G. DORAN, HEAD
SOLID STATE PHYSICS

DONALD L. BENEDICT, DIRECTOR
POULTER RESEARCH LABORATORIES

Reproduction in whole or in part is permitted for any purpose of the United States Government

Copy No. 19

FOR OFFICIAL USE ONLY

DISCLAIMER NOTICE

THIS DOCUMENT IS BEST QUALITY PRACTICABLE. THE COPY FURNISHED TO DTIC CONTAINED A SIGNIFICANT NUMBER OF PAGES WHICH DO NOT REPRODUCE LEGIBLY.

OR are
Blank pgs
that have
Been Removed

BEST AVAILABLE COPY

ABSTRACT

Peak pressure calibration, pressure-time profile response tests, and pressure-resistance hysteresis of the Manganin in C-7 epoxy transducer are described. It is shown that predicted and measured pressure-time profiles agree to within 10 percent. Also presented are: the transformation of profile measurements from transducer to test specimen, Hugoniot temperature calculations for C-7 epoxy up to ~500 kbar peak pressure, a method of constructing gages of Manganin in conducting materials, and gage field test results on the FLAT TOP series of events.

CONTENTS

CONTENTS

ILLUSTRATIONS

ILLUSTRATIONS

TABLES

I INTRODUCTION

A. GENERAL

Current activity in underground nuclear detonations has generated considerable interest and consequent research in the shock propagation properties of rocks and soils. Laboratory measurements typically determine the Hugoniot characteristics of proposed shot media, which are used in field test predictions of stress-time and stress-distance profiles. Field instrumentation has been developed to measure the latter,[1] but the former has been difficult to achieve. In fact, stress-time profile measurements of explosively produced shock waves, even on a laboratory scale, have been limited to short duration and, depending on the type of transducer, to rather narrow stress ranges.[2,3]

The objective of the investigation discussed in this report is the development of a piezoresistive transducer or system of transducers capable of measuring stress-time profiles in rocks and soils. Specific response goals are short rise time, < 0.1 μsec, long duration recording, > 50 μsec, and an overall stress accuracy of ± 10 percent in a stress range from 10 kbar to as high as possible, preferably at least 500 kbar.

Since the primary goal of this work is a transducer system for field measurements, fundamental investigations of the piezoresistive effect in conductors under dynamic compression have been examined only with respect to the goals outlined above. Although preliminary studies of resistivity *vs.* peak pressure have been made for several alloys, peak pressure calibration, pressure-resistance hysteresis, shock heating, etc. have been studied for only one type of alloy, Driver-Harris Manganin,* and one specific wire size, 0.003 inch diameter. Except for peak pressure calibration, the measurements have been made in a somewhat cursory manner in that only a few experimental tests of each type have been performed, whereas more quantitative results would require a statistical determination and much more elaborate techniques. These would result in major investigations in themselves.

---

* Driver-Harris Co., Harrison, N J., Nominal Composition, 84% Cu, 12% Mn, 4% Ni.

It should be noted that the investigations reported below have been performed in isotropic, homogeneous media with plane shock waves and analyzed using one-dimensional shock wave theory. The departure from these conditions in actual field tests may be appreciable due to geological faults and inhomogeneities in the region of transducer placement. The effect of these unideal conditions on transducer response can be estimated, at present, in only a very qualitative manner and has not been undertaken in the present work. Therefore, field test results in which flow in the vicinity of the transducer departs greatly from one dimensionality must be regarded as qualitative also. This does not include spherical divergence from a "point source" detonation since, in general, the measurement is made at a sufficiently large radius so that divergence can be neglected.

B. BACKGROUND

Prior work in the field of high dynamic stress transducers has been reviewed briefly in a previous report[4] and in Reference 1. Similarly, requirements for and selection of piezoresistance transducer components have been outlined and reported.[4,5] In essence, this work led to the selection of D-H Manganin alloy and C-7 epoxy* as the resistive and insulator elements, respectively, of a high-stress transducer. The response characteristics of this transducer formed a major portion of the ensuing investigation. In particular, investigations of transducer pressure-resistance hysteresis, peak pressure calibration, and effects of insulator electrical and shock properties were examined. It was found that all these could be measured experimentally with the exception of insulator shock heating. Preliminary calculations showed that C-7 temperatures may be as high as 500°C at 150 kbar peak pressure.

The work reported in the following sections is an extension and refinement of the work areas outlined above. One additional area of effort is described: matching the shock characteristics of the gage to that of proposed shot media by (1) decreasing the compressibility of the gage insulator and (2) imbedding the Manganin directly in samples of the proposed media.

---

* Armstrong Products, Inc., Warsaw, Indiana

The purpose of this report is primarily to describe the response of the Manganin in epoxy transducer with respect to the tests performed on it and will therefore include portions of work reported previously. In addition, the most recent gage configurations and test results are described. Section II presents a summary of work performed since the report of Reference 4; Section III, a brief discussion of some aspects of the results; Section IV A describes the shock characteristics of C-7; and Appendix A and B, the C-7 Hugoniot temperature calculations; IV B, the shock response of Manganin; IV C the Hugoniot matching work; IV D, recent transducer configurations; IV E, recording circuits; and IV F, field test work.

II SUMMARY

Response of the Manganin in epoxy transducer has been extended to ~ 290 kbar peak pressure calibration and ~ 150 kbar hysteresis calibration. Constant pressure (ambient) measurements have been made of the temperature coefficient up through the melting temperature, ~ 1020°C. The transformation from transducer profile recordings to profiles in adjacent test materials has been examined by the method of characteristics. For the numerical example chosen, C-7 epoxy on aluminum, the distortion caused by the presence of gage is small. Hugoniot temperature calculations, completed for C-7 epoxy, show epoxy temperatures reaching ~ 2500°K at 500 kbar. Wire temperature calculations as a function of time have not been completed.

The feasibility of making profile measurements directly in limestone, granite, and tuff with a Manganin wire has been demonstrated. Complete Manganin response characteristics in these media have not been determined; however, measurements of peak pressure were about as expected. An insulator-Manganin foil assembly has been used successfully in an aluminum block configuration to record peak pressure and profile for ~ 1 μsec. The mechanism of failure after this time has not been determined.

III DISCUSSION

A. GENERAL

A transducer capable of recording shock wave stress-time profiles must necessarily respond to very high frequency changes in mechanical stress. Consequently, stress wavelengths are generally much less than transducer dimensions, and the shock wave response of the individual transducer components determines not only the overall transducer response but also the actual profile being measured. Such is the case with Manganin wire in C-7 epoxy, shown schematically in Fig. 1(a) and pictorially in 1(b). The wire is the transducing element, and the surrounding C-7 insulator acts as a pressure transformer between a test specimen and the wire. The stress-time profile recorded depends on the shock properties of the insulator as well as the piezoresistive response of the wire.

Ideally, the insulator should behave as a fluid of low electrical conductivity. Measurements of transducer response and C-7 equation of state reported in the following sections indicate that, within experimental error, C-7 behaves ideally up to at least 150 kbar. Measurements above this pressure indicate a possible change in slope in the shock velocity-pressure velocity curve. Frequently this is indicative of a phase transformation of a material and is characterized in the pressure-time profile as a double wave.[6] However, a double-wave structure has not been observed in C-7, although both free-surface velocity[7] and transducer records have been recorded up to ~290 kbar.

Assuming the epoxy does behave as a fluid, the Manganin wire peak pressure calibration, which has been obtained principally in C-7 epoxy, must be considered as applicable only when the wire is under dynamic hydrostatic pressure. Should the wire be used in a material in which the stress is anisotropic, the response may be altered; static pressure measurements on Manganin have indicated this to be true.[8] Dynamic measurements in which the anisotropy is known have not been performed; however, these may now be possible with the transducer configurations described in Section IV D. In fact, the universality of these transducers may depend on knowing the response of Manganin to anisotropic stress.

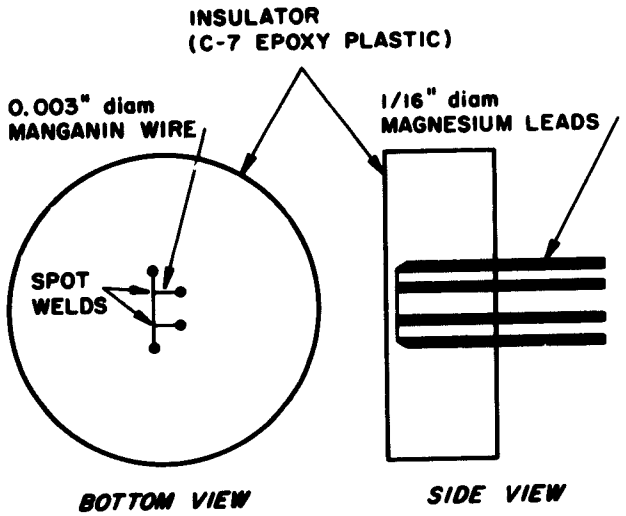

(a) TRANSDUCER CONFIGURATION

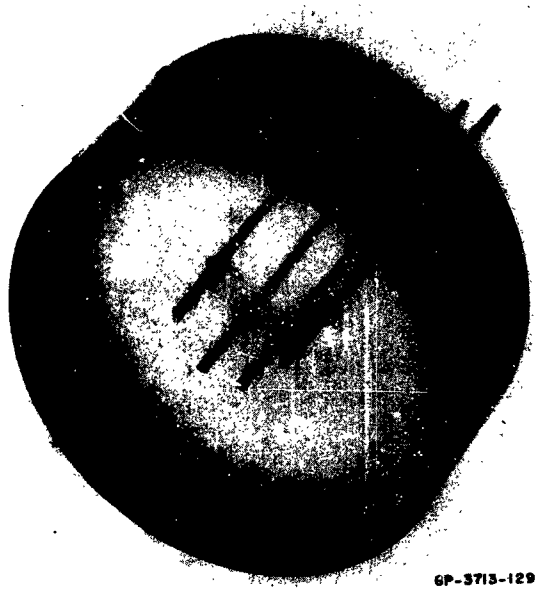

(b) PICTORIAL VIEW

FIG. 1 MANGANIN IN C-7 EPOXY TRANSDUCER

By referring the Manganin peak pressure calibration to the epoxy pressure, there is one additional restriction: the results may be valid only for the particular method by which the pressure is obtained, *i.e.*, a single shock in C-7. Experiments with Manganin in other insulators, notably doped epoxy, have yielded calibration values within the experimental error of those obtained with C-7. However, the compressibilities, and hence the paths by which the final P-V-E (pressure-volume-energy) states are reached have been very similar to C-7. Two possible exceptions are the Hi-D glass results, reported under "Peak Pressure Calibration," and Manganin in aluminum, reported under "Additional Gage Development." To date, sufficient data have not been generated to distinguish between scatter and a change in the pressure coefficient in either system when compared to C-7; however, this will be studied further, both theoretically and experimentally.

Values of pressure-resistance hysteresis have been determined for the combination of wire in epoxy. Pressure cycling was performed by shock compression and subsequent unloading by relief wave reflection from a free surface. Since the expansion under these conditions is adiabatic,[6] the epoxy and wire do not return to prestressed temperature and volume. Possible contributions of the residual temperature to measured hysteresis values have been assumed negligible since zero-pressure temperature coefficient measurements indicate insignificant resistance change, $<-2\%$, up to approximately the Manganin melting temperature. To the extent that measurements apply after pressure cycling, the quoted hysteresis values can be considered applicable to Manganin.

B. TRANSDUCER APPLICATION

It was mentioned above that the Manganin in C-7 transducer measures a profile existing in the C-7 insulator. The corresponding peak pressure and pressure profile in an adjacent test material depend on the shock impedances and equations of state, respectively, of the two materials. A transformation in peak pressure can be readily accomplished by the well-known impedance match procedure if the appropriate cross characteristics of the materials are known.[9] A pressure-time profile transformation is somewhat more complex, depending on the quantity desired; that is, the profile measured by the transducer is that existing at the test material-transducer interface. The profile in the test material is altered by the waves reflected from the interface. In field test work this effect is

not included in predicted profiles. Hence an estimate of the distortion caused by the gage is required. This can be accomplished for materials which behave as fluids by a calculation using the method of characteristics,[10] as outlined in Appendix A. A specific example (suitable for comparison with future measured profiles) of a given driver system was chosen for analysis. The general procedure is discussed first step by step to demonstrate the construction of a characteristic "net" from which appropriate pressures can be assigned to regions of an adjacent-test material as represented in distance-time (x, t) space.

For the materials used, the net effect of interaction of relief waves is a decrease in the rate of decay of pressure from that which would exist if the gage material were identical to the test material. In the example chosen, a true rate of decay (defined as that existing in an all aluminum system or if the gage insulator were matched to the aluminum) can be estimated by extending the unrefracted relief waves to the right in Fig. A-1 and through the plane of the (virtual) interface. Pressure *vs.* time at the epoxy-aluminum interface and at the virtual interface, as determined from gage data, are given in Table I. Here the time increments in column 2 result from the arbitrarily chosen time increments,

Table I

PRESSURE-TIME PROFILE DISTORTION RESULTS

PRESSURE (kbar)	TIME OF RELIEF WAVE ARRIVAL (μsec)	
	Aluminum, C-7 Interface	Aluminum, Aluminum Interface
148	0	0
140	0.44	0.42
129	0.84	0.80
117	1.30	1.23
106	1.61	1.53
96	2.00	1.85
90	2.39	2.30
79	2.77	2.69
69	3.16	3.01

0.4 μsec, used in the analysis of Appendix A. Zero time refers to shock arrival at the aluminum C-7 interface. The time intervals shown in column 3 are those obtained graphically without the gage present, *i.e.*,

in an all aluminum medium. It can be seen that the difference is less than the desired 10% accuracy set as a gage goal. For this particular example, distortion in the profile caused by the presence of the gage would be small. For estimates of other materials, the Hugoniots and relief adiabats, from which the sound velocity can be computed, must be known.

IV EXPERIMENTAL PROCEDURE AND RESULTS

A. SHOCK CHARACTERISTICS OF C-7 EPOXY

Since the integrity of the Manganin in C-7 transducer depends greatly on the characteristics of the C-7, it is necessary that these be examined in considerable detail. The procedure followed in the present work has been first to measure the C-7 Hugoniot equation of state; then, by using these data, to calibrate the Manganin wire for peak pressure response, hysteresis, etc. In addition, since shock heating accompanies shock compression, a program was initiated to calculate Hugoniot temperatures and possible effects on wire resistance. Temperature calculations at pressures up to 500 kbar have been completed; calculations of wire temperature as a function of time have not been started.

1. Hugoniot Measurements

The Hugoniot of C-7 has been reported previously[4] for pressures up to 150 kbar. This has been extended to 220 kbar by conventional "in contact" explosives and to 290 kbar by flying plate techniques.[11] A complete summary of Hugoniot data is presented in Table II. The data up to ~170 kbar can be represented by an equation of the form:

$$P = 0.07816\mu + 0.1956\mu^2 + 0.2214\mu^3 \text{ (mbar)}$$

where

$$\mu = \frac{\rho}{\rho_0} - 1, \quad \rho_0 = 1.19 \text{ g/cc} \quad . \tag{1}$$

A fit in the range from 170 to the highest pressure obtained, 370 kbar, has not been made because of insufficient data.

2. Hugoniot Temperature Calculations

Shock loading of the Manganin wire imbedded in expoxy causes a change in wire temperature due to direct shock heating and conduction heating from the surrounding epoxy. Since a pressure profile and not a pressure-temperature profile is desired, an estimate of epoxy temperature and its

Table II

SUMMARY OF C-7 HUGONIOT DATA

PRESSURE (kbar)	U_s (mm/μsec)	U_p (mm/μsec)	METHOD
37.7	3.86	0.83	F.S.* wedge
40.9	3.97	0.87	
45.9	4.06	0.95	
51.0	4.15	1.03	
55.5	4.24	1.10	
60.3	4.34	1.17	
65.4	4.42	1.24	
70.4	4.51	1.31	
75.4	4.60	1.38	
81.0	4.60	1.45	
57	4.38	1.12	Imp. match (Al)
	4.33		
145	5.76	2.14	Imp. match (Al)
274.5	7.19	3.24	F.S., F.P.†
74	4.70	1.33	F.S.
74	4.70	1.33	Imp. match (Mg)
170	6.2	2.34	Imp. match (Mg)
170	6.2	2.34	F.S.
175	6.34	2.39	Imp. match (Mg)
190	6.34	2.57	F.S.
237	6.79	2.99	F.S.
225	6.79	2.88	Imp. match (Mg)
370	7.88	3.98	F.P., F.S.
368	7.88	3.98	F.P., Imp. match (Al)
293	8.06	3.09	F.P., F.S.
259	6.46	3.39	F.P., F.S.
20.7		0.49	Gage, assuming k = 0.29%/kbar

* Free surface velocity.

† Flying plate.

effect on the wire is necessary. Calculations of the temperature-time profile in the wire are being made in two steps; calculation of epoxy Hugoniot temperatures and conduction heating of the wire by the epoxy. The first has been completed and is outlined in Appendix B. The calculation is made by assuming that the epoxy equation of state can be represented by the Mie-Grüneisen equation with the zero pressure Grüneisen constant, Γ, calculated from elastic and thermal properties. At elevated pressures, values of Γ are used which are obtained from one measurement and its estimated limits of error. (See Appendix B.) An isentrope centered at the foot of the Hugoniot is calculated by an iterative process from the measured Hugoniot and several values of Γ. Hugoniot temperatures are then generated by using values of specific heat at constant volume which were calculated from specific heat measured isobarically as a function of temperature. The applicability of the Mie-Grüneisen equation of state to

C-7 plastic and the dependence of the specific heat on volume are not known. However, the calculations were made to obtain only an estimate of plastic shock temperatures from which wire temperature could be calculated and are felt to be sufficient for this purpose.

Results of the Hugoniot temperature calculations are shown in Fig. B-5. The significance of the various values shown for Γ and the regions labeled I and II are explained in Appendix B. It can be seen that epoxy temperatures are apparently high even at modest pressures, being $\sim 1000^{\circ}K$ at 200 kbar.

3. Electrical Properties

In general, the conductivity and charge generation measurement techniques outlined in Reference 4 have been applied to the extended pressure range up to 290 kbar. An exception is a parallel plate method in which a more quantitative value of conductivity was obtained. The configuration is shown in Fig. 2(a).

Any polarization disturbances induced on one plate must likewise be induced on the other because the plates are identically positioned with respect to the shock front. The external circuit provides nearly identical paths to ground from each plate, and consequently polarization-induced signals in the direction of shock propagation will not be present in V_{12}, the voltage displayed on the scope. V_{12} is proportional to the current which flows through the sample because of the applied voltage. This yields the resistance of the sample from which the resistivity may be easily computed.

Another pair of plates is placed near the first pair and is connected to a similar external circuit; however, no voltage is applied to the sample. This circuit is monitored as a check on the polarization signals produced normally to the direction of shock propagation.

An experiment with this arrangement has been performed using C-7 epoxy plastic as the insulator and aluminum foil plates 5 mm by 15 mm with a separation of 1 mm. This gave a resistance of $1.9 \times 10^{5}\ \Omega$ at 140 kbar immediately after shock front passage and corresponds to a resistivity of $1.6 \times 10^{12}\ \mu\Omega$cm, neglecting fringing effects at the edges of the plates. (Inclusion of a correction for fringe effects would raise this figure slightly.) Thus the quoted value is a minimum resistivity which, when compared to the resistivity of Manganin, $\sim 48\ \mu\Omega$ cm, is essentially infinite.

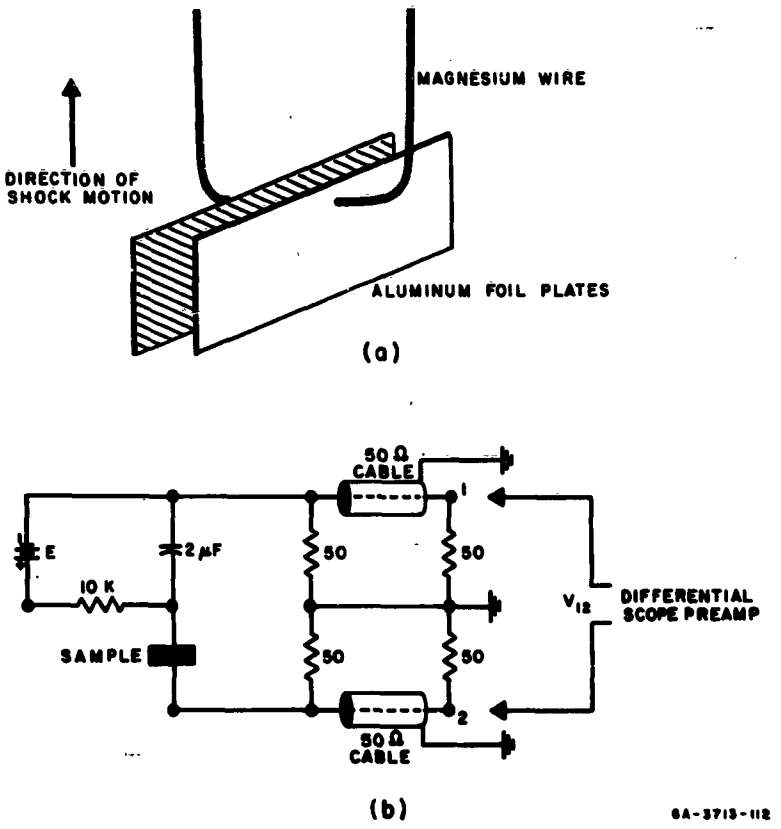

FIG. 2 INSULATOR RESISTIVITY MEASUREMENT
(a) Electrode Configuration
(b) Circuit Schematic

Induced currents in the Manganin wire, attributed to epoxy dipole reoreintation under shock loading, have been observed in transducer records during shock transit through the epoxy prior to reaching the wire. Hauver[2] has investigated this phenomenon extensively in polar plastics and has generated quantitative data relating induced currents to peak pressure. In the present work induced currents are < 4 percent of the measuring current at the highest calibration pressure obtained, 290 ± 30 kbar.

Induced currents, while small, do create some difficulty in the measurement of Manganin resistance change. The measurement is made with a constant current power supply system (see Section IV E); however, induced currents cause a change in current just prior to shock arrival. This

appears on transducer records as a small step preceding the pressure wave. In the present work it has been assumed that the current at the instant of shock arrival is the sum of power supply and induced currents. Any error introduced by this assumption is relatively small, as can be seen from the order of magnitude of the current as quoted above.

B. SHOCK RESPONSE OF MANGANIN

1. Manganin-Hugoniot Equation of State

The Hugoniot equation of state of Manganin has been measured previously[4] up to 359 kbar peak pressure. The results are included here (Table III) for comparison with the piezoresistance data presented in Table IV and curve of Fig. 3. It can be seen that there are no indications of a phase change (characterized by an inflection point in the Hugoniot[6]). A phase change would raise the possibility of a discontinuity in the pressure-resistance relationship. Peak pressure calibration reported below has shown no discontinuity over essentially the same pressure range.

2. Peak Pressure Calibration

The resistance of Manganin as a function of peak pressure has been measured principally for one alloy, Driver-Harris (nominal composition, 84% Cu, 12% Mn, 4% Ni). A summary of similar work on other Manganin alloys has been presented elsewhere.[12] The results discussed below pertain only to the Driver-Harris alloy.

In a pressure range from 20 to 200 kbar, "in contact" explosive driver systems have been used to generate dynamic pressures. A typical assembly of this type is shown in Fig. 4. A range of peak wire pressures was obtained by using insulator and driver plate materials of different shock impedances, by using high explosives of different Chapman-Jouget pressures, and by varying the explosive pad thickness and hence the peak pressure attenuation due to the Taylor relief wave. The majority of work has been done with one insulator, C-7 epoxy, since the change in resistance of Manganin with pressure has not yet been shown to be independent of the internal energy state of the Manganin at a given pressure. For this reason, peak pressure *vs.* resistance values are considered uniquely determined by the method by which the peak pressure was obtained; for example, direct

Table III

HUGONIOT DATA, MANGANIN ALLOY,

ρ_0 = 8.46 g/cc

PRESSURE (kbar)	SHOCK VELOCITY (mm/μsec)	PARTICLE VELOCITY (mm/μsec)	RELATIVE VOLUME $1 - (V/V_0)$	METHOD OF OBSERVATION
56	4.02	0.165	0.041	Free surface (inclined mirror)
107	4.36	0.294	0.067	Impedance match
157	4.52	0.413	0.091	Free surface (inclined mirror)
254	4.88	0.616	0.126	Free surface (inclined mirror)
346	5.15	0.780	0.150	Free surface (inclined mirror)
360	5.18	0.820	0.159	Free surface (inclined mirror)

Table IV

PRESSURE-RESISTANCE DATA
MANGANIN WIRE

PRESSURE (kbar)	INSULATOR	DIRECT (D) OR REFLECTED (R) SHOCK	$\Delta R/R_0$ (%)						PRESSURE SOURCE
			SHOT NO.	Oscilloscope No.				$\Delta R/R_0 \pm \sigma$ %	
				1	2	3	4		
20 ± 1	C-7	D	A	6.0	--	--	--	5.7	Light gas gun
24 ± 2		D	A	7.0	6.8	6.7	--	7.0 ± 0.5	"In contact" explosive
			B	6.7	6.8	6.7	--		
59 ± 2		D	A	16.9	--	--	--	16.9	
74 ± 2		D	A	20.6	--	--	--	20.6	
134 ± 4		D	A	38.6	--	--	--	38.6	
166 ± 5		D	A	47.0	--	--	--	47.0	
169 ± 5		D	A	47.0	--	--	--	47.0	
175 ± 5		D	A	48.1	--	--	--	48.1	
212 ± 5		D	A	55.7 54.6	52.7 51.5	51.4 50.9	51.7 51.4	52.9 ± 1.7	
			B	58.4 56.5	53.8 53.4	55.5 54.5	-- --	55.3 ± 1.9	
220 ± 6		D	A	55.3	--	--	--	55.3	
120 ± 5		R	A	32.9	--	--	--	32.9	
281 ± 10		R	A	74.7	--	--	--	74.7	
360 ± 30		R	A	80.4	--	--	--	80.4	
135 ± 5	Hi-D glass	D	A	32.9	--	--	--	32.9	
279 ± 10		D	A	61.5	--	--	--	61.5	
129 ± 8	Aluminum*	D	A	31.6	--	--	--	33.2 ± 1.4	
			B	34.6	--	--	--		
			C	31.6	--	--	--		
			D	34.5	--	--	--		
			E	33.3	--	--	--		
290 ± 30	C-7	D	A	69.0	--	--	--	69.0	Flying plate

* See Section IV D

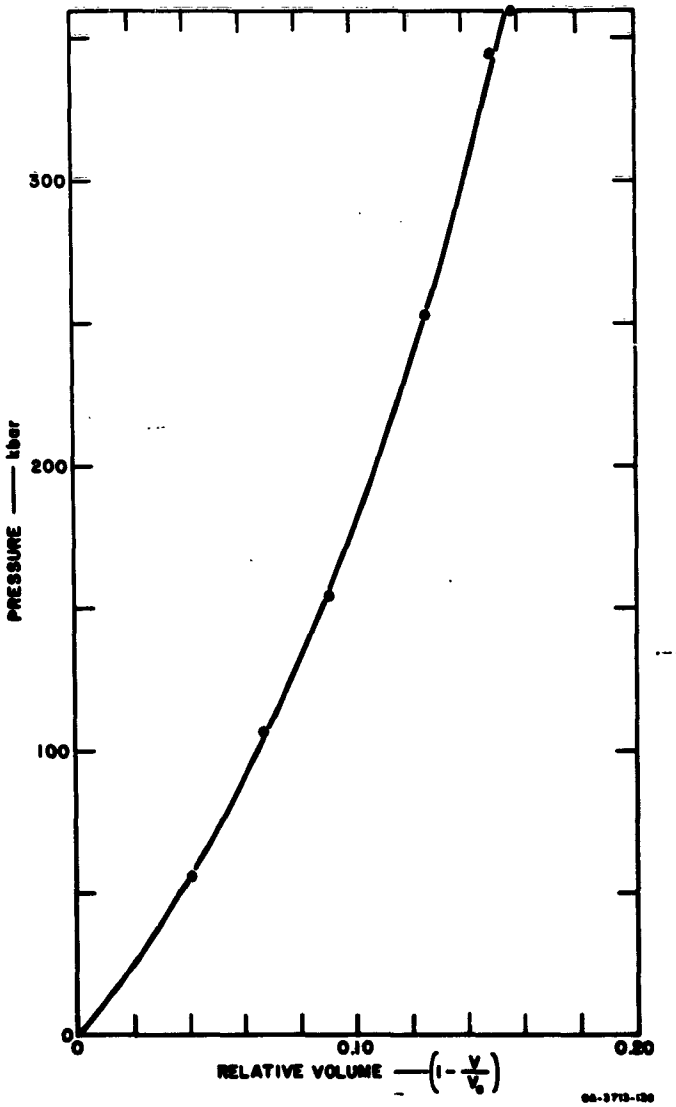

FIG. 3 MANGANIN HUGONIOT, ρ_0 = 8.46 g/cc

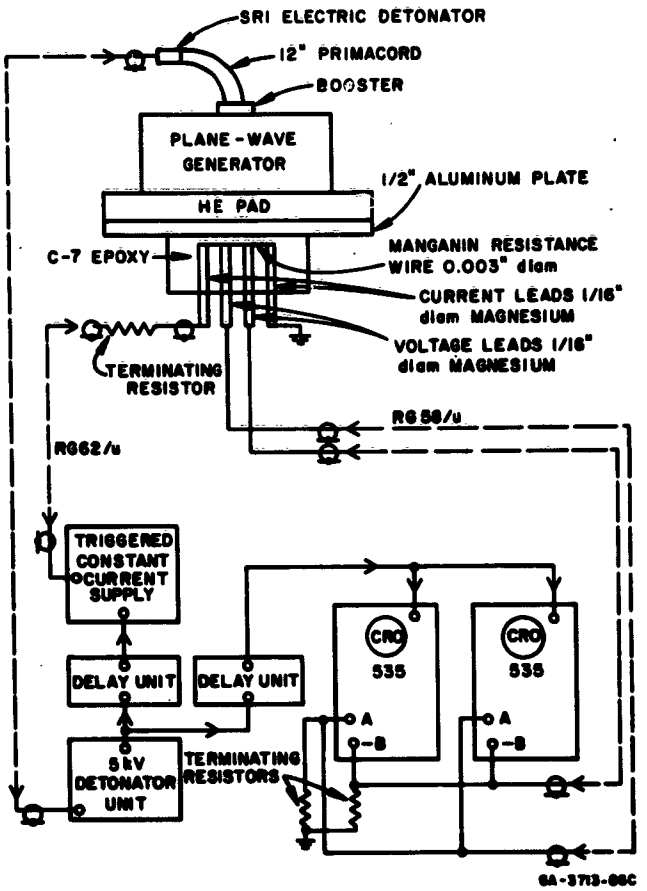

FIG. 4 SCHEMATIC CONFIGURATION OF DRIVER SYSTEM, TRANSDUCER, AND RECORDING CIRCUITS

shock *vs.* reflected shock, and also according to the medium in which the wire was imbedded. The results of the most recent calibration shots are presented in Table IV and the curve of Fig. 5.

Calibration pressures have been determined by measuring insulator pressures by either the impedance match procedure or a free surface-shock velocity measurement.[7] The Manganin wire is placed as close to the plane of free-surface velocity measurement or to the driver plate-insulator interface as possible, usually within 1 mm. In this way, errors introduced by peak pressure attenuation are minimized.

The calibration of Manganin in C-7 as a transducer is statistical in that the transducer is, of course, destroyed in use. A brief discussion of the reliability of the calibration as well as accuracy is therefore appropriate.

In general, it was found that if several wires were imbedded at the same plane in C-7 epoxy, the change in resistance agreed to within the reading accuracy of the recording oscilloscopes. Under the best conditions; that is, with large percentage changes in resistance, this accuracy was ±1.5 percent, deteriorating to ±5 percent at the lowest resistance change. The accuracy of the corresponding pressure measurement varied inversely with pressure, being typically ±5 percent at the low pressures and as high as ±10 percent at the highest direct shock pressure reached.

The pressure points above 220 kbar listed in Table IV were obtained, as indicated, by one or a combination of several techniques; flying plates, reflected shock wave, and Hi-D glass, or aluminum media. The technique used in the aluminum shots will be discussed in Section IV D. In the case of the flying plate shots, the tabulated result represents one successful shot out of three attempts. In this one shot, although two separate transducers gave resistance changes within 3 percent, optical measurements of free-surface and shock velocity yielded the large uncertainty shown. This ambiguity in optical measurements resulted from the non-planar shock arrival. The pressure error limits shown are based on errors incurred in data reduction.

The reflected wave shot yielded more consistent results, although a comparison with direct shock values can not be made at this time, because of the uncertainty in the PVE states, as described above. The configuration of these shots is shown in Fig. 6. The peak pressure of the brass

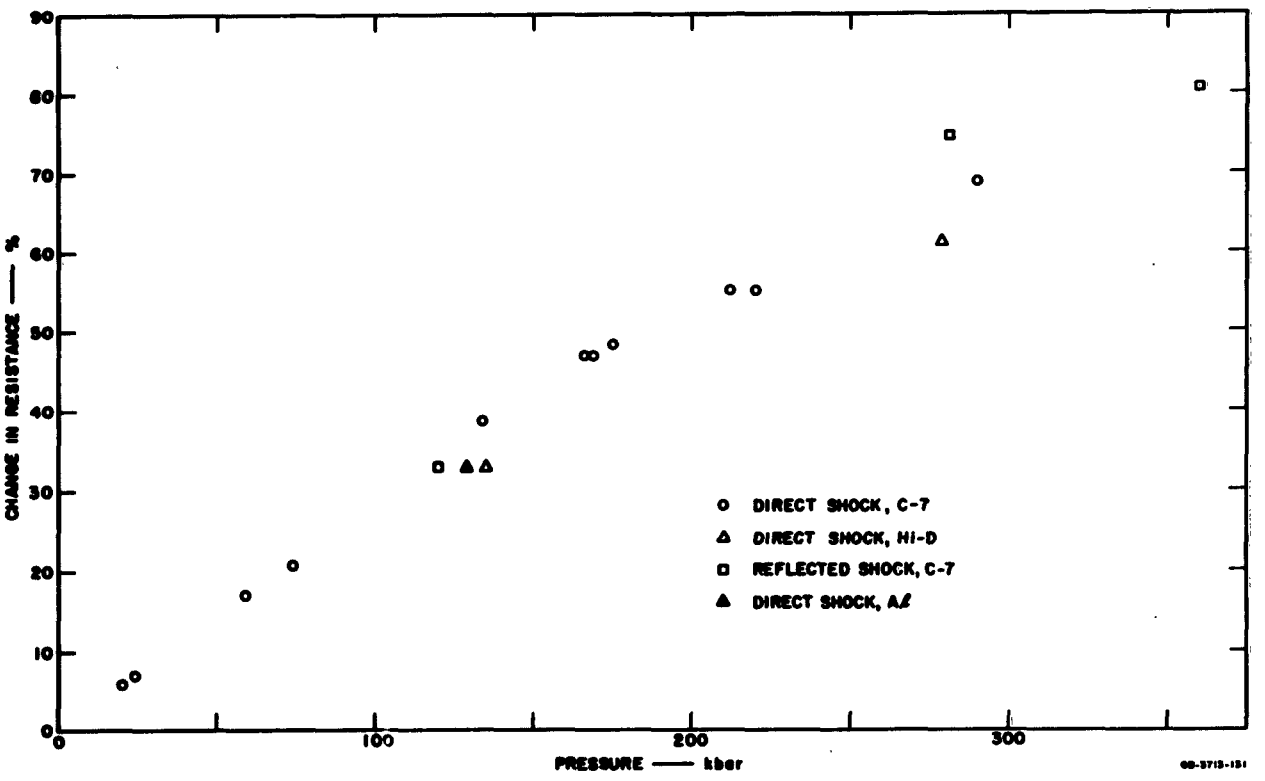

FIG. 5 CHANGE IN RESISTANCE AS A FUNCTION OF PRESSURE, D–H MANGANIN WIRE

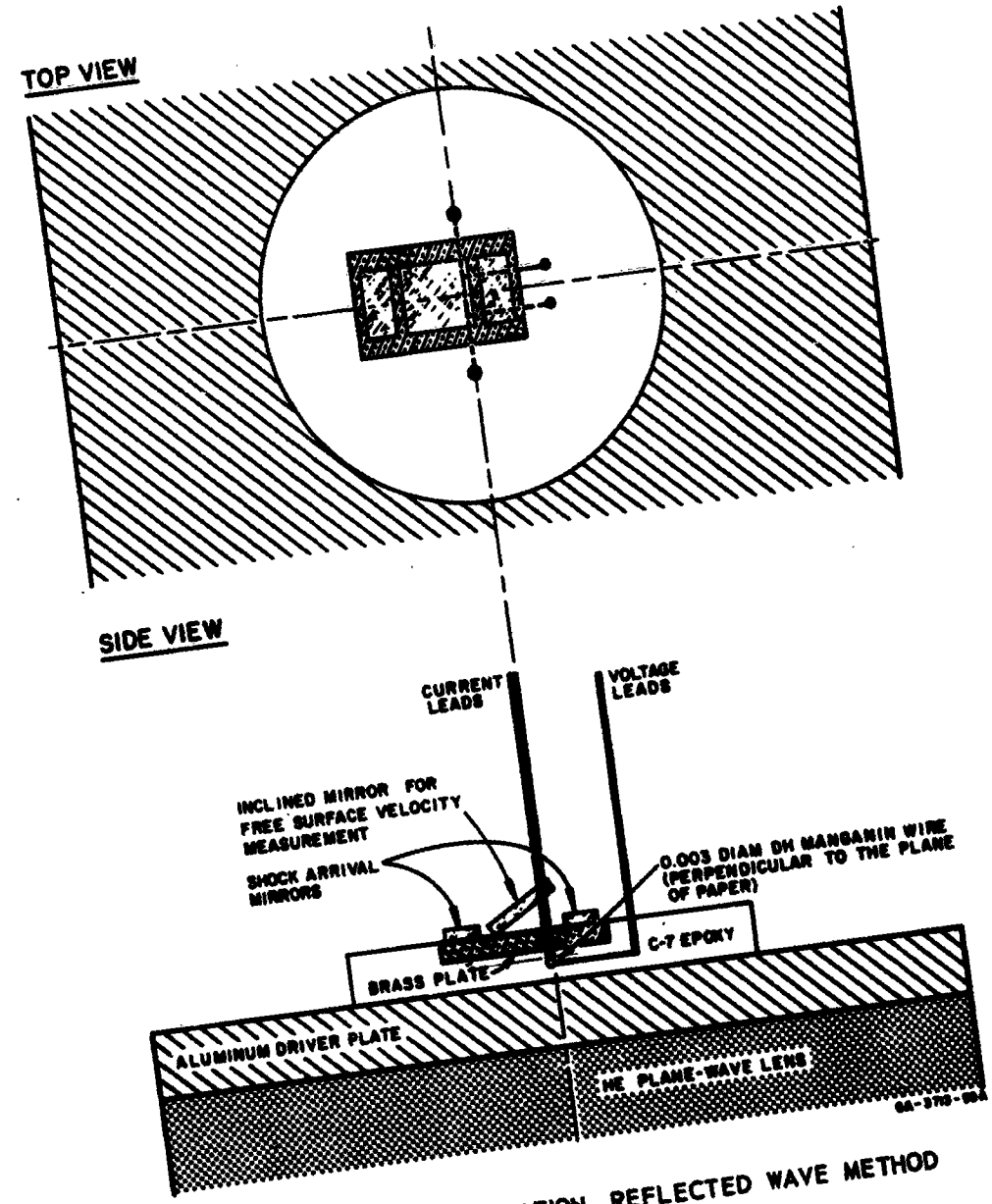

FIG. 6 TEST CONFIGURATION, REFLECTED WAVE METHOD

backing-plate was obtained by a free-surface velocity measurement from which the C-7 pressure was obtained by an impedance match procedure. Attenuation in the reflected and incident wave, both in the C-7 and in the thin brass plate, has been neglected for two reasons: the close proximity of the wire to the epoxy-brass interface and the slow rate of change of pressure *vs.* time as indicated by the wire record.

It can be seen from the curve of Fig. 5 that, for the direct shock epoxy points, there appears to be a change in slope occurring in the region of 150 kbar. The reflected wave and Hi-D data, although limited, do not show this. It is suspected that the change in slope may be due to the epoxy and not the Manganin; however, C-7 Hugoniot results do not reflect this. Considerably more data and more accurate pressure measurements are required to resolve the pressure-resistance dependence of Manganin further. Within the accuracy desired for field gages, the change in resistance of Manganin with peak pressure in C-7 epoxy and under direct shock loading can be represented by:

$$\frac{\Delta R}{R_0}(\%) = k_1 \cdot P(\text{kbar}) \text{ for } P < \sim 150 \text{ kbar} \qquad (2)$$

$$= 0.16 + k_2 \cdot P(\text{kbar}) \text{ for } 150 < P \leq 290 \text{ kbar} \qquad (3)$$

where

$$k_1 = 0.29 \pm 0.02 \text{ (\%/kbar)}, \quad k_2 = 0.18 \pm 0.01 \text{ (\%/kbar)} .$$

The nominal value of k_1 is about 4 percent less than that previously quoted.[4,12] The principal reason for this is a change in the recording system (explained in Section IV E) to permit more accurate results and higher frequency response.

3. Temperature Dependence of the Pressure Coefficient

The entent to which wire heating, either directly by shock or through conduction from the insulator, affects the measured resistance change is difficult to determine. Static pressure measurements[13] have indicated that the effect is negligible. Dynamic measurements, reported previously,[4] have been indirect in that wire heating was accomplished before shock compression, whereas to simulate actual conditions in an insulator, heating should be performed after shock compression. The results reported in Reference 4

show that up to 500°C and 145 kbar the pressure coefficient is independent of temperature within experimental error. Recent work has not extended this measurement but has been confined to measuring the ambient pressure temperature coefficient up through the melting point of Manganin (~1000°C), thereby obtaining at least an indication of its behavior. The results are shown in the resistance *vs.* temperature curve of Fig. 7. The largest change in resistance observed up to the melting point was ~−2 percent. The change in resistance between 500°C, the temperature reached in the above referenced work, and melting temperature is negligible. Consequently, on the basis of the ambient pressure temperature coefficient, there is no indication of a change in the pressure coefficient with temperature, *i.e.*, in shock-loading Manganin, no change in the coefficient due to an increase in temperature by shock heating is expected. Similarily, if the ambient pressure temperature coefficient can be applied to elevated pressure results, it would be expected that conduction heating of the wire would not alter the pressure-induced resistance-time profile until perhaps

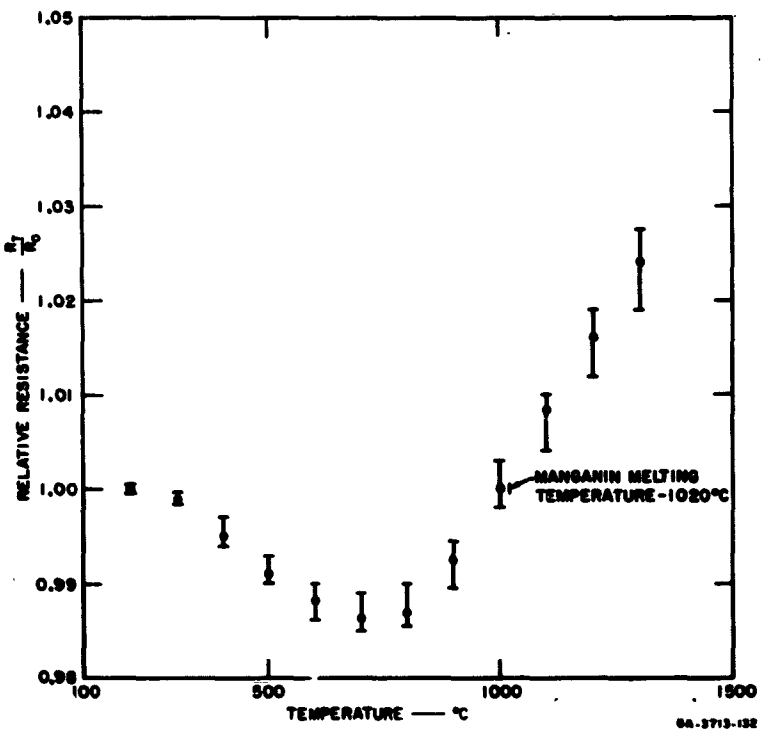

FIG. 7 RESISTANCE AS A FUNCTION OF TEMPERATURE, D–H MANGANIN ALLOY

the melting temperature of Manganin were reached. Since this is likely to be well above the zero-pressure value[14] and is difficult to predict, and since conduction heating has not yet been calculated, the actual effect of temperature can only be inferred from the above mentioned results and measured profiles reported below.

4. Pressure-Resistance Hysteresis

Static pressure work with Manganin has shown the pressure coefficient to decrease slightly with repeated pressure cycling until a stable value is reached.[15] In addition, the static pressure coefficient measured for increasing pressure is within a few percent of that measured for decreasing pressure.[16] These static measurements were made isothermally although separate temperature cycling has shown a stablizing effect on the pressure coefficient.[15] In shock wave studies it is more difficult to isolate and to measure a purely pressure-resistance hysteresis effect since wire compression is accomplished by shock heating and expansion occurs adiabatically. Moreover, measurements performed in an insulating medium are influenced by the thermal properties of the insulator.

The hysteresis results reported here have been made with respect to the Manganin and C-7 epoxy insulator as a combination. Two principal methods have been used: 1) subjecting wire and epoxy to a sudden known decrease in pressure shortly after peak pressure, and 2) comparing the pressure-time curve recorded in test shots with one calculated from pressure-distance data measured on the same shot. It is thought that in the case of a step decrease, the wire expansion is adiabatic, *i.e.*, the wire is insulated from the epoxy, whereas in the slowly decaying wave heat is conducted to the wire from the epoxy. However, conduction calculations have not yet been made. In both cases, described below, measurements, although few, have been sufficient to establish the magnitude of the hysteresis effect.

The experimental system for generating a step decrease in pressure is shown in Fig. 8. It is similar to the reflected wire shots except that materials of lower shock impedance were placed immediately behind the sensitive length of wire (between voltage taps, see Section IV E).

Two series of shots have been conducted: pressure cycling Manganin in C-7 to various peak pressures and subsequent relief to atmospheric, and pressure-cycling Manganin in doped epoxy insulators (see Section IV C) to

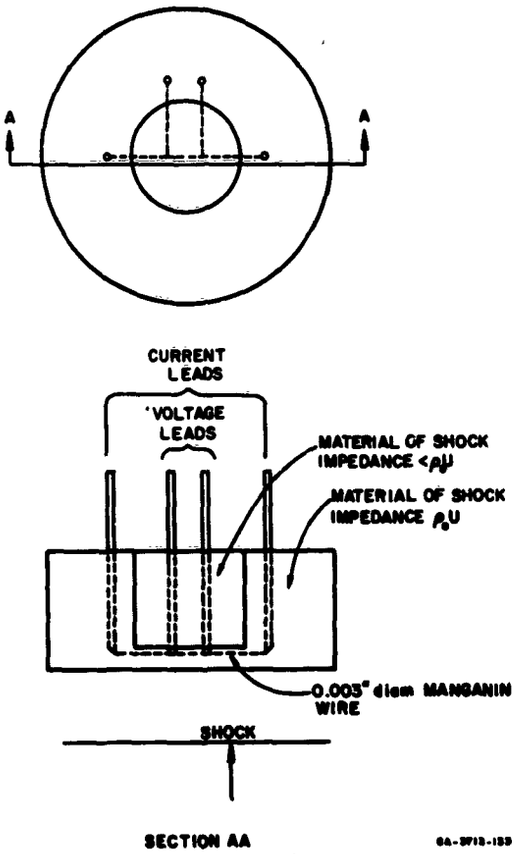

FIG. 8 TRANSDUCER CONFIGURATION, RELIEF WAVE SHOTS

various peak pressures and relieving to intermediate pressures by means of C-7 epoxy backing. The results are shown in Tables V and VI. The intermediate pressure results are less accurate than those at zero pressure for two reasons: peak pressure and relief pressure values are subject to the rather large uncertainties in the Hugoniots and relief adiabats of the doped epoxies, and quoted values of measured decreasing pressure change were obtained by using a pressure coefficient obtained

Table V

RELIEF WAVE CALIBRATION DATA, INTERMEDIATE PRESSURES

INSULATOR		MEASURED $\Delta R/R$ (%)	MEASURED $-\Delta P$ (kbar)	EXPECTED $-\Delta P$ (kbar)
1	2			
67% Si, 33% C-7	C-7	7.3	23	26
67% Hi-D, 33% C-7	C-7	5.8	19	17
77% Hi-D, 23% C-7	C-7	13.1	42	47
77% Hi-D, 23% C-7	C-7	17.4	56	50

Table VI
RELIEF WAVE CALIBRATION DATA, ZERO PRESSURE

PEAK PRESSURE (kbar)	HYSTERESIS % OF PEAK ΔR	HYSTERESIS % OF R_0
58	11.9	2.0
59	9.2	1.6
98	9.1	2.5
108	10.0	3.1
133	10.8	4.1
137	15.1	5.9
147	15.5	6.5

for increasing pressure change. It has not yet been shown that the two are equivalent. However, the intermediate pressure results do indicate that hysteresis is insignificant compared to a 10 percent accuracy goal.

The zero-pressure relief wave shots show a definite change in zero-pressure resistance after pressure cycling. This change appears to be a function of peak pressure as shown in Fig. 9. The changes in resistance have not been corrected for possible residual temperature effects since measurement of the temperature coefficient of resistance, outlined above, indicates the correction to be negligible. The magnitude of the residual change after cycling to 150 kbar approaches the desired overall accuracy of the transducer system. Additional work of this type is required to obtain more quantitative results and to extend the range of measurement.

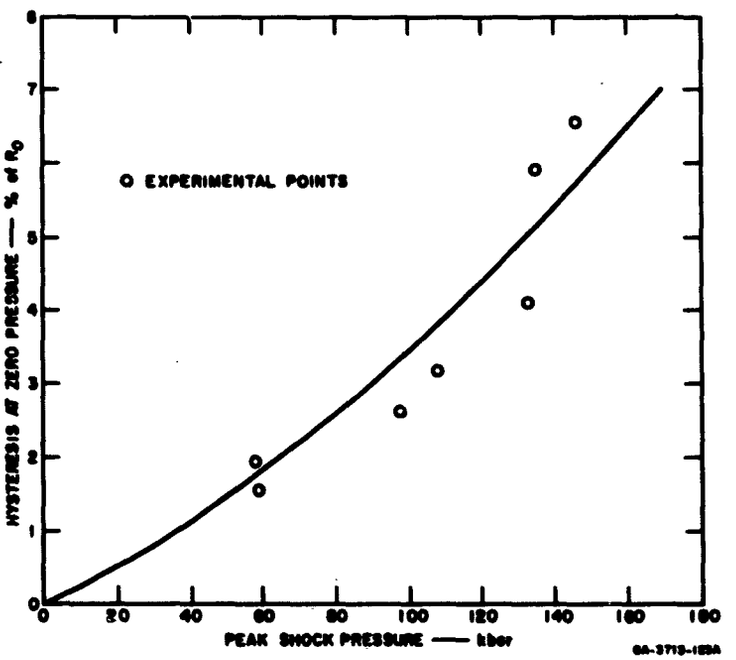

FIG. 9 PRESSURE–RESISTANCE HYSTERESIS OF MANGANIN

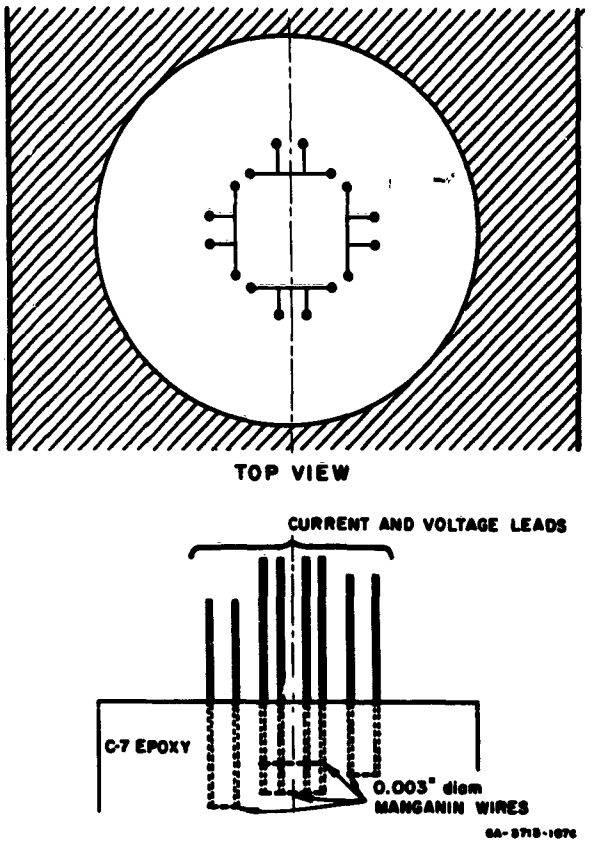

FIG. 10 CONFIGURATION OF P(t), P(x) SHOTS

Response to a gradually decaying wave has been examined by the system shown in Fig. 10. By using several wires spaced a known distance apart in the direction of shock propagation, the measured pressure-time profile at any wire can be compared with the profile calculated from peak pressure decay with distance as measured by subsequent wires.

This can be clarified by reference to Fig. 11, distance *vs.* time, where at time t_0, the shock front is at plane x_0 and peak pressure is P_0. At time t_1, the front has moved to x_1, and the peak pressure is now P. There is a distance behind the shock front where the relief wave pressure is P. If we call this distance coordinate x_p and corresponding time coordinate t_p we can solve for t_p as follows:

$$t_1 - t_p = \frac{x_1 - x_p}{u_p + a} \qquad (4)$$

and

$$t_p - t_0 = \frac{x_p - x_0}{\bar{u}_{p0}} \tag{5}$$

where u_p is the mass velocity, a is the local sound velocity at pressure P, and $\bar{u}_{p0}$ is the average mass velocity between x_0 and x_p.

Since

$$x_1 - x_0 = \bar{U}_s(t_1 - t_0) \tag{6}$$

where $\bar{U}_s$ is the average shock velocity between x_1 and x_0, adding (4) and (5) and equating to the right hand side of (6) gives

$$t_p = t_1 \frac{(\bar{U}_s - u_p - a)}{(\bar{u}_{p0} - u_p - a)} \tag{7}$$

Subsequent wires measure a peak pressure and a corresponding average shock velocity, $\bar{U}_s$. Values of $\bar{u}_{p0}$ are known from Hugoniot data. The

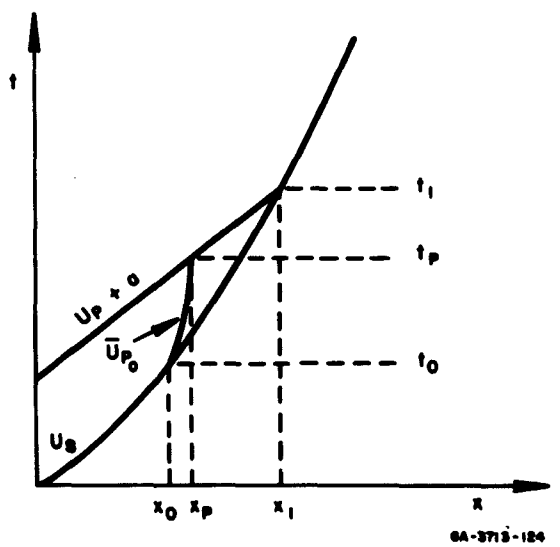

FIG. 11 DISTANCE–TIME DIAGRAM, RELIEF WAVE CALIBRATION

sound speed, a, can be calculated from the difference in slope between the Hugoniot and adiabat at a given pressure, P, and volume, V, as given by[6]

$$a^2 = c^2(1 - \Delta) \quad , \tag{8}$$

where a is the adiabatic sound speed, $c^2 = dP/d\rho$ along the Hugoniot and Δ is defined by:[6]

$$\Delta = \frac{\Gamma}{2} \rho(V_0 - V)[1 - (U - u_p)^2/c^2] \tag{9}$$

Γ = Grüneisen ratio = $V/c_v(\partial p/\partial T)_v$, c_v is the specific heat at constant volume.

V = specific volume $\cong 1/\rho$ cc/g

U = shock velocity at P, V

u_p = mass velocity at P, V.

The ratio of c/a as a function of pressure for C-7 epoxy is shown in Fig. 12.

Three shots were made with a gage configuration as shown in Fig. 10, two at ~180 kbar peak pressure in the first wire and one at ~63 kbar peak pressure. In all shots the difference between measured and calculated profiles for each wire was not greater than 10 percent. A tabulation of predicted and measured values for one of the high pressure shots is shown in Table VII, where $P_{n,r}$ is the predicted pressure at wire, n, from peak pressure measurements at wire, r, etc., and P_n is the measured pressure at time, $t + n$, determined by the procedure outlined above. The longest interval available for comparison is under 2 μsec. Longer times require

Table VII

$P(t)$ DATA DETERMINED FROM $P(x)$ MEASUREMENTS, EIGHT-INCH PLANE WAVE LENS (P - 80) PLUS 1-INCH COMP B PAD

WIRE NO.	PEAK PRESSURE (kbar)	$P_{n,r}$ (kbar)						P_n (kbar)	$t_n + n$ (μsec)
		$P_{1,2}$	$P_{1,3}$	$P_{1,4}$	$P_{2,3}$	$P_{2,4}$	$P_{3,4}$		
1	182	157	127	117	127	117	117	159	0.58
								131	1.12
								105	1.71
2	157							137	0.58
								119	1.16
3	127							113	0.60
4	117								

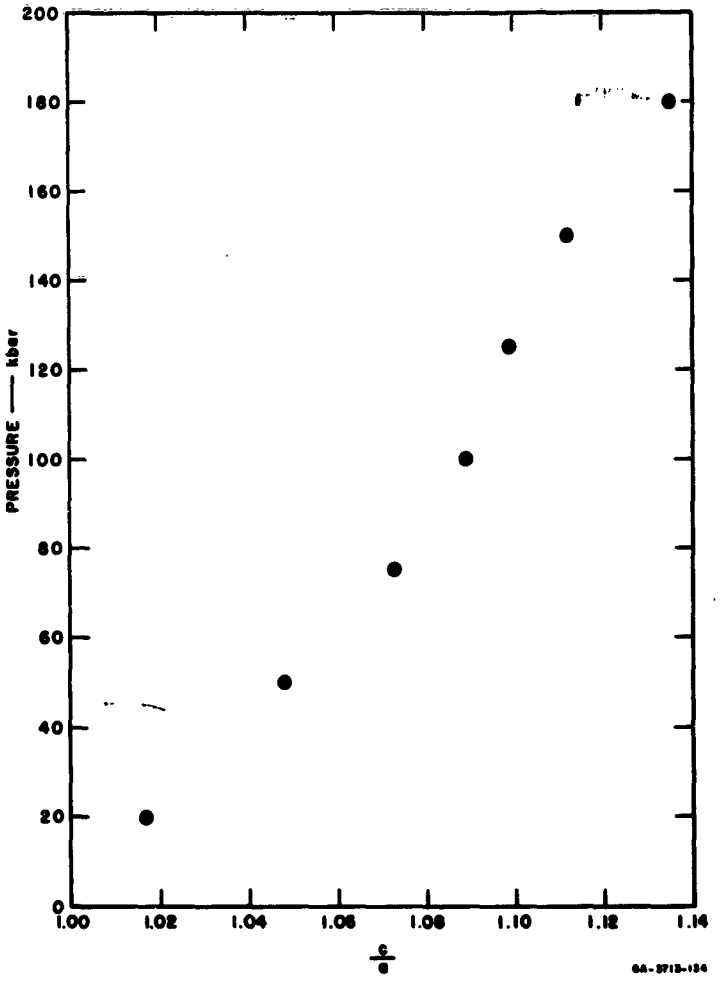

FIG. 12 RATIO OF "HUGONIOT" TO ADIABATIC SOUND VELOCITY AS A FUNCTION OF PRESSURE, C-7 EPOXY

a prohibitively large plane-wave explosive system to prevent lateral relief waves from distorting the profile. However, the measured response is within the desired accuracy.

C. HUGONIOT MATCHING

1. General

Although the majority of equation of state measurements have been on C-7 epoxy, Hugoniot points have been obtained on a number of other less compressible insulators. The goal of this work has been to provide a spectrum of transducer insulators of shock characteristics closely matched to expected field test environments. The initial work[4] was directed toward matching shock impedances to reduce peak pressure and pressure profile errors introduced by uncertainties in the shock characteristics of proposed test media. The work reported below has been directed toward matching transducer insulator compressibilities to those of its surroundings. By doing this, it is expected that distortionless recording for long durations can be achieved since disturbances originating at gage lateral boundaries will be eliminated. Two methods have been pursued: adding less compressible materials to expoxies ("doped" epoxies) and constructing transducers from native field shot media.

2. Hugoniot Matching

To accomplish Hugoniot matching, a method of predicting compressibilities of mixtures as a function of pressure is first required. From this, it is possible to obtain an expression for the compressibility-pressure relationship required of an additive to a given epoxy in order to obtain a given Hugoniot. Since considerable Hugoniot data had been generated on doped epoxies,[4] the data were fitted to existing synthesis methods to determine their applicability to mixtures. This portion of the work has been completed and is presented below. The results have not been applied to predicting the compressibility characteristics of materials required to match shot media.

The method of Lyakhov[17] as described by Chabai[18] appears to work reasonably well when applied to Hi-D in C-7 and W in C-7. As described in Reference 17, the mixture compressibility at a given pressure is assumed equal to the sum of the constituent compressibilities. A weighting

factor for each constituent is used according to constituent volume in the mixture, *i.e.*,

$$\eta(P) = \sum_{i=1}^{N} K_i \cdot \eta_i(P) \tag{10}$$

where P is shock pressure, $\eta = \rho/\rho_0$, the ratio of shocked to unshocked density, and K is the volume weighting factor. For the two-component epoxy system, the mixture compressibility $\eta_M(P)$ equals

$$\eta_M(P) = K\eta_E(P) + (1 - K)\eta_A(P) \tag{11}$$

where M, E, and A refer to mixture, epoxy, and additive material, respectively.

The results obtained with W in C-7, Hi-D in C-7, and SiO_2 in C-7 are shown in Table VIII. The calculated shock velocities of the mixture are obtained from the Rankine-Hugoniot conservation equations[19] and in this case are given by

$$U_s = \sqrt{\eta(P - P_0)/(\rho - \rho_0)} \tag{12}$$

The summation appears to yield good correlation between U_s and $\rho_0 U_p$, calculated and observed, for W in C-7 and Hi-D in C-7. In the case of SiO_2 in C-7, the equation of state of fused quartz was assumed to apply to the SiO_2 actually used. The correlation was fair but not so good as for the other two cases.

3. Limestone, Tuff, and Granite Transducers

Construction of transducers composed of native shot media has been accomplished for three materials, limestone, tuff, and granite. The general configuration is shown in Fig. 13. It consists of a block assembly cemented together with C-7 epoxy. A conventional four-lead (voltage and current), 3-mil-diameter Manganin wire assembly lies on the block marked No. 1 and under block No. 4. The voltage leads, Cu foils 0.004 inch thick × 0.125 inch wide, are brought to the cable end of the gage (top) between blocks Nos. 4 and 2 and similar current leads between blocks Nos. 3 and 4, and blocks Nos. 5 and 4. Shown also is a conductivity test foil extending from the plane of the wire to the cable end of the gage (between block Nos. 5 and 6).

TABLE VIII

CALCULATED AND OBSERVED VALUES OF U_s AND $\rho_0 U_s$

Material	ρ_0 (g/cc)	Pressure (kbar)	η_A	η_E	K	η_M	ρ (g/cc)	U_s (cm/sec × 10^5)		$\rho_0 U_s$	
								Cal.	Obs.	Cal.	Obs.
W in C-7	6.94	340	1.10*	1.94	0.682	1.670	11.6	3.48	3.55	24.2	24.6
	8.00	368	1.105	1.975	0.624	1.646	13.15	3.44	3.58	27.5	28.6
	6.95	100	1.03	1.48	0.682	1.339	9.3	2.39	2.48	16.6	17.2
	8.68	110	1.04	1.50	0.586	1.311	11.4	2.30	2.27	20.0	19.7
	6.96	38	1.015	1.265	0.682	1.187	8.26	1.87	1.83	13.0	12.7
	7.80	40	1.015	1.265	0.635	1.176	9.16	1.85	1.86	14.4	14.5
	9.33	145	1.045	1.570	0.550	1.335	12.45	2.49	2.56	23.2	23.8
	7.36	133	1.04	1.59	0.660	1.403	10.32	2.52	2.66	18.5	19.5
Hi-D in C-7	2.78	90	1.15	1.44	0.681	1.348	3.55	3.84	3.59	10.7	10.0
	2.58	86	1.15	1.44	0.721	1.362	3.52	3.53	3.52	9.1	9.1
	2.58	176	1.35	1.635	0.721	1.557	4.02	4.24	4.16	10.9	10.7
	2.58	204	1.37	1.685	0.721	1.592	4.11	4.46	4.20	11.5	10.8
SiO_2 in C-7	1.79	73	1.135†	1.40	0.495	1.268	2.27	4.41	3.92	7.9	7.0
	1.79	150	1.37	1.60	0.495	1.484	2.66	5.06	4.84	9.1	8.7

* Obtained from "Equation of State of Nineteen Metallic Elements from Shock-Wave Measurements to Two Megabars," R. G. McQueen and S. P. Marsh, *J. Appl. Phys.* 31, 1253-1269 (1960).

† Obtained from "Shock-Wave Compression of Quartz," J. Wackerle, *J. Appl. Phys.* 33, 922 (1962).

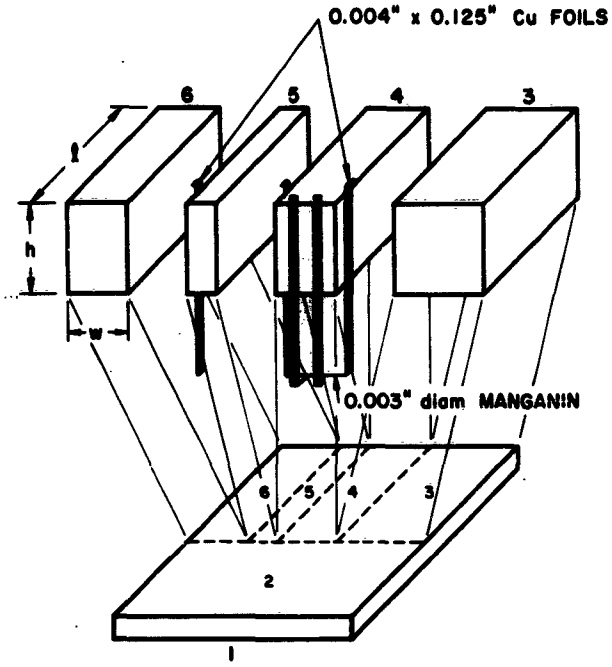

BLOCK DIMENSIONS — Inches			
NO.	w	h	ℓ
1	4	$\frac{3}{8}$	4
2*	4	$1\frac{1}{2}$	$1\frac{3}{4}$
3	$1\frac{1}{2}$	$1\frac{1}{2}$	$2\frac{1}{4}$
4	1	$1\frac{1}{2}$	$2\frac{1}{4}$
5	$\frac{1}{2}$	$1\frac{1}{2}$	$2\frac{1}{4}$
6	1	$1\frac{1}{2}$	$2\frac{1}{4}$

* NOT SHOWN

68-3713-122

FIG. 13 LIMESTONE BLOCK GAGE ASSEMBLY, SCHEMATIC VIEW

A pressure-time record from one limestone* shot using this assembly is shown in Fig. 14. The upper trace is that of the conductivity test probe with a 2-Ω external shunt resistor and associated constant current power supply. It can be seen that the limestone remains an insulator with respect to the 2-Ω shunt. The signal on the bottom trace is, therefore, that of the Manganin wire which is a direct measure of the pressure-time profile in the limestone.

In addition to the general success of recording directly in a rock material, there are several other noteworthy aspects of this particular test record:

(a) Records obtained from faster sweeping oscilloscopes show a two step rise, the first corresponding to a pressure of ~29 kbar and the second to a peak pressure of ~88 kbar. The separation between waves is <0.1 μsec.

* Spergen limestone, ρ_0 = 2.40 g/cc, 60% fossil fragments, 20% biocastic debris, 20% calcite; analysis from Ref. 20.

The first wave had not been detected in previous work with Spergen limestone,[20] although its existence was expected. Direct comparison of peak pressure results with previous work is difficult since the driver systems were not the same. However, the peak pressure of the second wave is about what would be expected from the limestone Hugoniot data of Gregson, *et al.*, and the cross curve of the explosive driver, Baratol. High sensitivity oscilloscopes (~1.5 kbar resolution) showed no elastic precursor wave, which is in agreement with the data obtained by optical techniques on similar thickness samples.

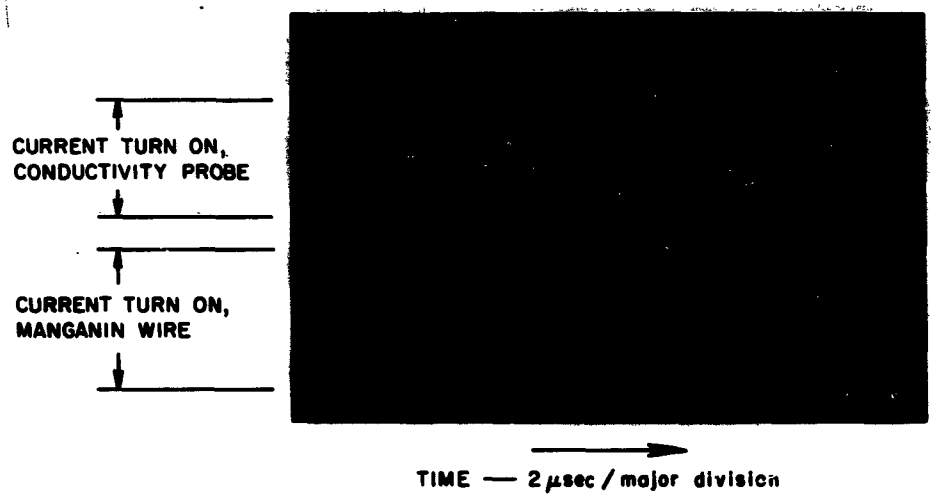

FIG. 14 RESPONSE OF MANGANIN IN LIMESTONE, PEAK PRESSURE ~88 KBAR

(*b*) The total recording duration (before wire breakage) was ~17 μsec. Stretching of the wire, manifested in the record as the first increase in voltage after initial peak, occurred after 6 μsec or approximately at the arrival time at the wire of the relief waves originating at the peripheral gage-air boundary. In effect, the wire assembly and leads moved in pressure and particle velocity equilibrium with the limestone, indicating that if this gage system were in an all limestone medium, the recording duration would be limited by the length of the limestone gage assembly.

A similar test on an all tuff* gage gave a record as shown in Fig. 15. The general construction was similar to that of Fig. 13 and is shown in

* NTS, area *U* 12B, ρ_0 = 1.4 g/cc.

FIG. 15 RESPONSE OF MANGANIN IN TUFF, PEAK PRESSURE ~ 56 KBAR

Fig. 16. A peak pressure of 56.4 ± 5 kbar was measured. The exact Hugoniot for this sample of tuff is not known; however, if Lombard's[21] curves for *U* 12*B* tuff are averaged, a pressure of 60 ± 6 kbar would be expected.

The records from two granite* gages are shown in Figs. 17 and 18. The general increase in noise over the limestone and tuff records is due to the granite and is thought to be a piezoelectric signal from the included quartz. From the records it can be seen that at the higher pressure, ~280 kbar, the conductivity of granite (measured by conductivity probe) increases (manifested as an apparent negative pressure, ~6 μsec after peak) to the same order of magnitude as that of the Manganin resistance wire and is therefore not useful as a gage insulator. These results have prompted work on a more universal gage system which is outlined in the next section.

Although the peak pressures measured by the wire in granite were approximately those expected from the granite Hugoniot,[21] peak pressures were not known sufficiently accurately to compare the Manganin response with Manganin in C-7 calibration.

* Hard Hat granite, Area 15 NTS, ρ_0 = 2.7 g/cc.

FIG. 16 MANGANIN IN TUFF ASSEMBLY, PICTORIAL VIEW

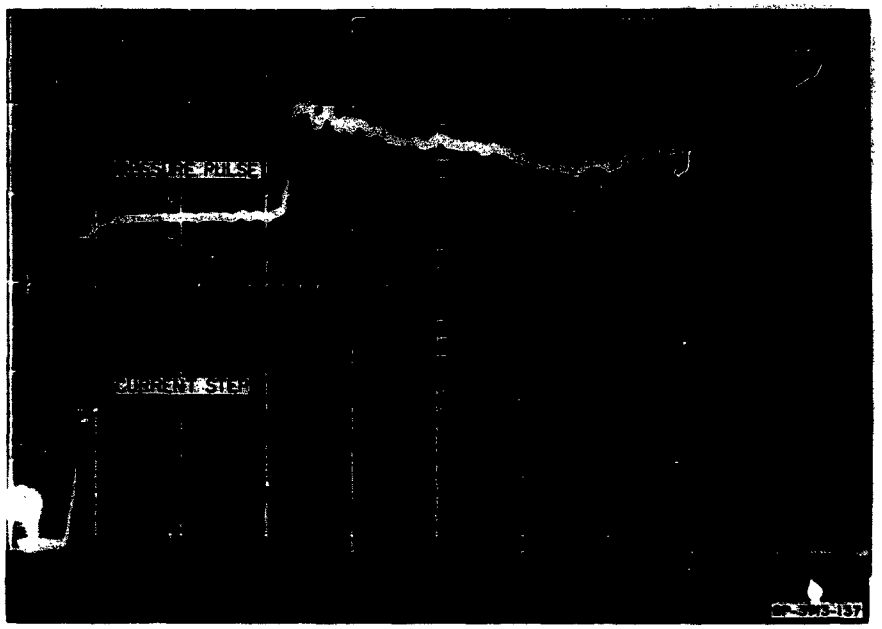

FIG. 17 RESPONSE OF MANGANIN IN GRANITE, PEAK PRESSURE ~100 KBAR

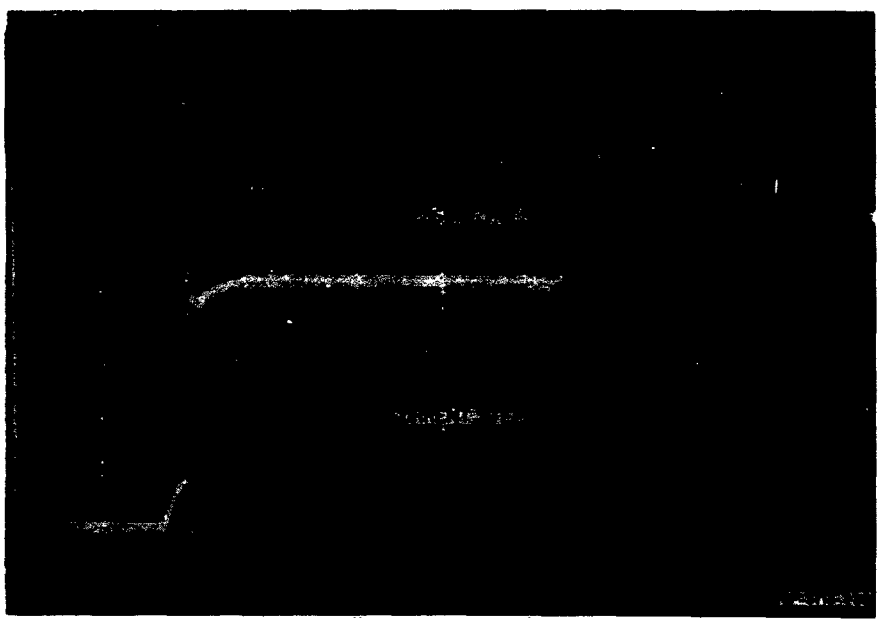

FIG. 18 RESPONSE OF MANGANIN IN GRANITE, PEAK PRESSURE ~250 KBAR

D. ADDITIONAL GAGE DEVELOPMENT

The ability to measure pressure-time profiles within a material, rather than at a free surface, is advantageous to laboratory as well as to field tests. The preceding results with Manganin in various materials have shown that, if the test specimen is an insulator, transducers can be constructed from them and an apparently reliable profile measured. However, should the material become a conductor under shock loading the transducer obviously fails. Several methods have been tried to insulate the wire from its surroundings and yet maintain the block construction. In all trials, aluminum has been used as the test material because it is a conductor of well-known equation of state, thereby permitting simultaneous measurements of the configuration and of the Manganin peak-pressure calibration in a medium other than C-7 epoxy.

FIG. 19 MYLAR–MANGANIN–MYLAR FOIL ASSEMBLY

The configuration shown in Fig. 19 was found to be satisfactory for short duration recording, <1 μsec. It is constructed by compressing the standard four lead, 0.003-inch-diameter Manganin wire assembly (see Fig. 1) into a thin ribbon, 0.001 inch thick. The ribbon is placed between ~0.0013-inch-thick Mylar films and the assembly compressed between heated (110°C) anvils. The total thickness of the Mylar-Manganin-Mylar assembly is slightly more than the thickness of the original Manganin wire and, accordingly, has a comparable rise time. Although Mylar has been interposed in the system, it is assumed that the equilibrium time of the assembly is sufficiently short, <0.1 μsec, to cause no perturbations in the shock profile.

The results of one aluminum block-foil assembly are shown in Fig. 20. The nature of the failure after ~0.8 μsec has not yet been determined. However, variations of this basic assembly have yielded recording durations

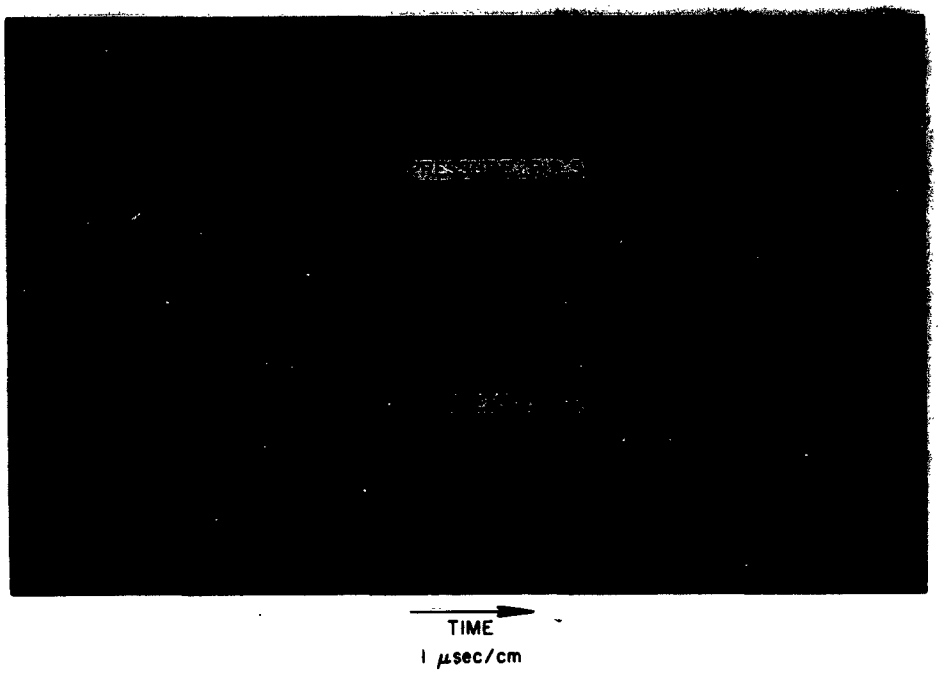

FIG. 20 RESPONSE OF MANGANIN–MYLAR FOIL IN ALUMINUM, PEAK PRESSURE ~117 KBAR

up to ~7 μsec, about the limit imposed by the particular overall dimensions used. The fidelity of recording after peak on these transducers has not been measured.

E. RECORDING CIRCUITS

Standard high frequency pulse techniques have been observed in the recording circuits shown in Fig. 4. The change in Manganin resistance is measured by a four-terminal system, two voltage leads and two current leads. The use of a four-lead system minimizes errors introduced by the possible change in resistance at the junction of the wire and current posts. Effectively, the measured change in resistance is that between the voltage taps, which permits measurements to be confined to the center region of the wire only; an example is the case of the reflected wave shots of Section IV B.

A constant current power supply (Fig. 21) minimizes errors due to stray inductance. The supply is triggered just prior to shock arrival at

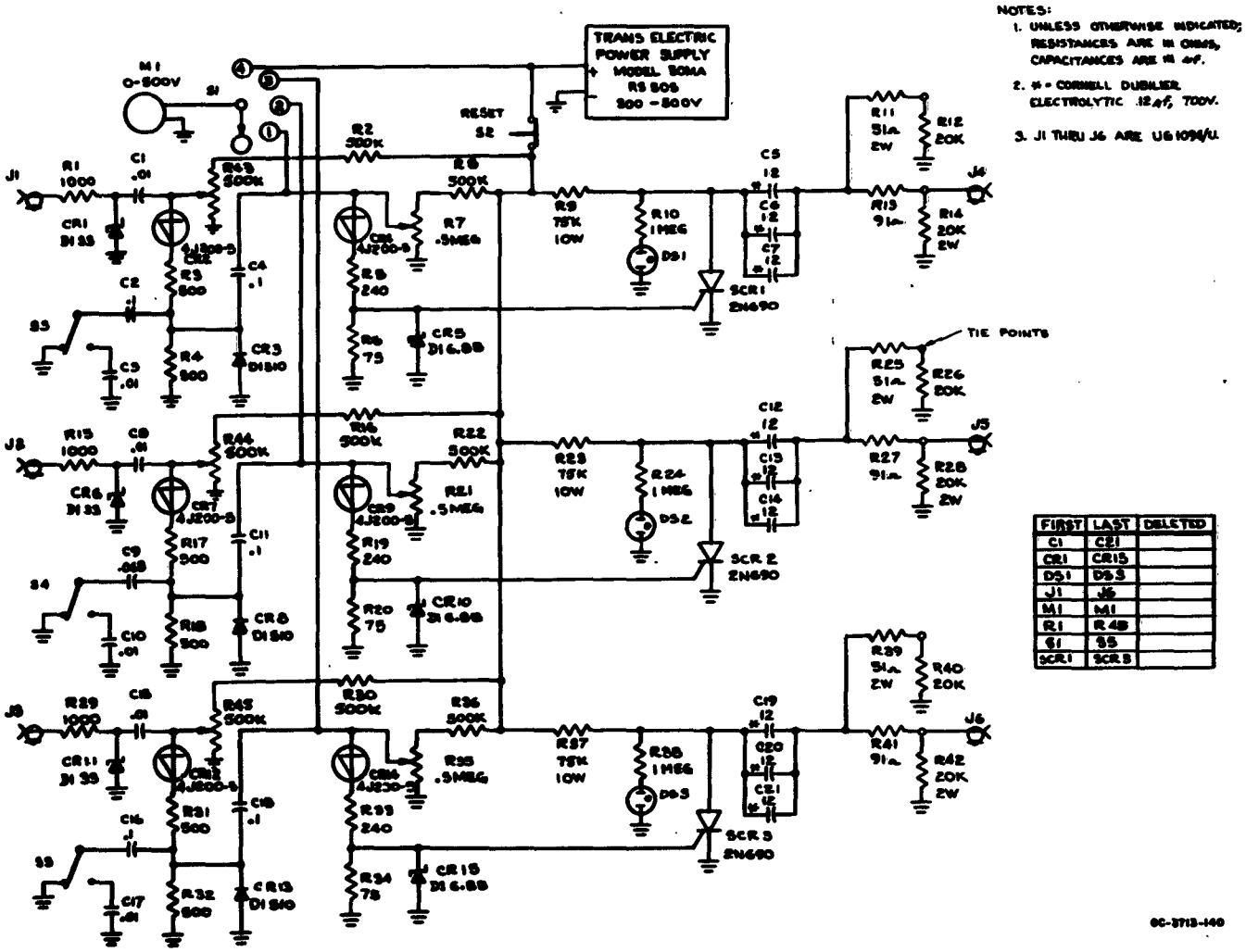

FIG. 21 SCHEMATIC — TRIGGERED CONSTANT CURRENT POWER SUPPLY

the wire to allow display of the current turn-on signal. This signal appears as a voltage step, V_0, which is proportional to the initial wire resistance, R_0, and is followed by a voltage step, ΔV, proportional to the change in resistance ΔR, at the time of shock arrival. With this method, the necessity of voltage and current calibration is eliminated. The actual quantity measured, $\Delta V/V_0$, is related to $\Delta R/R_0$ by

$$\frac{\Delta R}{R_0} = \frac{\Delta V}{V_0} + \beta \quad , \tag{13}$$

where β accounts for the slight change in wire current due to the parallel resistances of the differential voltage circuits. Values of β *vs.* $\Delta V/V_0$ are shown in Fig. 22. For field use the correction is insignificant but must be considered in the peak pressure calibration discussed in Section IV B.

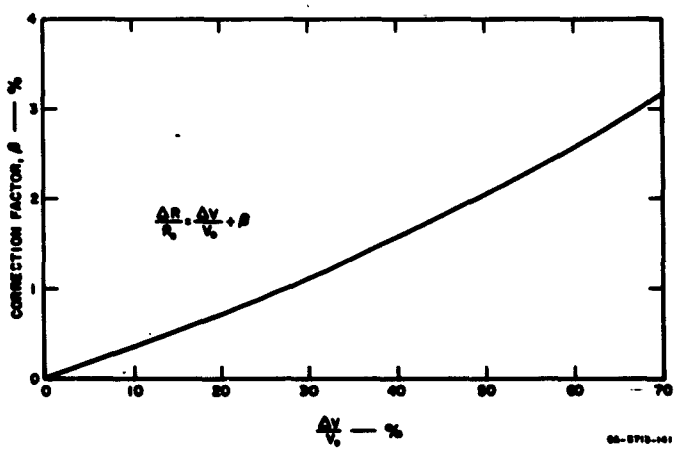

FIG. 22 RECORDING CORRECTION FACTOR β, vs. $\Delta V/V_0$

The differential recording system provides the normal benefits of common mode rejection, thereby assuring measurement of only the change in resistance of the center portion of the wire. However, care must be taken in the system balance; for example, in the voltage dividers formed by the voltage tap series and termination resistors. Although it is not a problem in laboratory tests, field tests require more careful cable balance.

F. FIELD TESTS

1. General

Early field tests are reported in Reference 4. More recent tests have been conducted in conjunction with the FLAT TOP series of events to provide fielding experience with various gage and trigger systems. All transducers were of the Manganin in C-7 configuration. Since the Hugoniot of the surrounding medium was generally not known, the recorded pressure profiles have not been related to the surrounding medium. The transducer results of each event are described below in chronological order. Recording and overall performance results are described in another report.[22]

2. Flat Top II

In this test conducted in playa, a 50-Ω transducer[4] using a bridge circuit[4] was placed ~6 inches from the source (TNT)-sand interface. Since the shock tilt and shock properties of the reconstructed medium in the immediate vicinity of the gage were not known, the pressure amplitude results are of dubious value. However, the function tests of the gage and recording systems were successful.

The records are shown in Fig. 23. Curve "*a*" is a reproduction of the actual trace recorded, in which the pressure pulse occurred just at the end of the power supply turn-on signal. Because the gage signal appeared early, it can be concluded that there was considerable shock tilt and that the shock wave reached the PZT piezoelectric trigger probe, placed three inches in front and on top of the gage, just shortly prior to reaching the gage. These conclusions are substantiated by the relatively slow rise time of the gage signal. The "true" recorded pressure-time profile, shown as curve "*c*," can be obtained from the baseline shift during this interval, curve "*b*"; fortunately, this was recorded prior to the shot. The peak pressure recorded was 30.4 ± 1 kbar. Approximately 7.5 μsec after shock arrival, the gage wire began to stretch due to the peripherally originating relief waves. After ~30 μsec, the wire was seen to break. The mismatch between gage and soil is not known, as the soil was hand-tamped around the gage. It is noteworthy that the gage remained intact in this environment for a considerably longer time than a similar shot in air; *i.e.*, although the arrival time of the relief wave is nearly the same, the amplitude, as might be expected, is considerably less. As pointed out previously, the

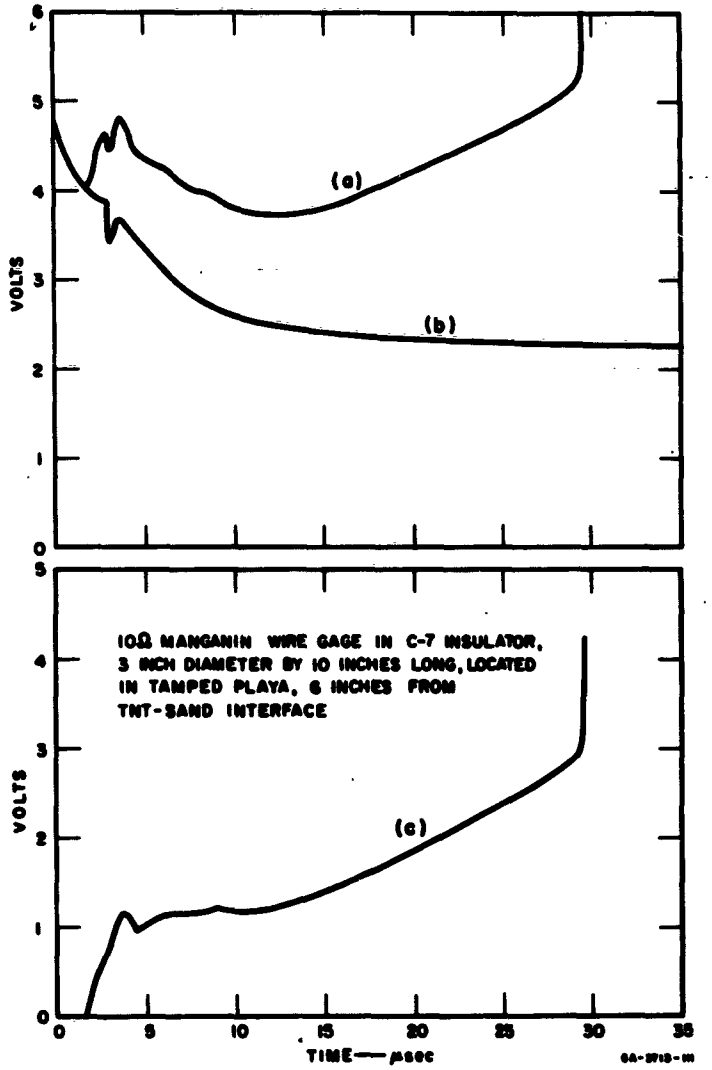

FIG. 23 PRESSURE–TIME PROFILE, FLAT TOP II

gage is measuring a profile which exists in the gage insulator and which departs from the profile in the surrounding medium at some time after peak pressure, depending upon the gage dimensions.

3. Flat Top III

a. GAGE CONFIGURATION AND PLACEMENT

Four Manganin wire gages, three 1-Ω differential and one 50-Ω, were placed abutting native playa at distances of 53, 60.5, 78, and 94.5 inches from shot center. Closest distances to a TNT surface turned out to be on the order of 2, 6, 26, and 42 inches, respectively. The general placement configuration is shown in Fig. 24(a) and (b), the recording schematic in Fig. 25, and a typical 1-Ω differential gage in Fig. 26. This gage was constructed to provide a 20-μsec duration recording at 100 kbar and was identical, except in diameter and thickness, to standard laboratory gages. The 50-Ω gage was a self-triggering unit constructed for a previously scheduled NTS test. The power supply circuitry for each type has been described in detail elsewhere.[4]

b. RESULTS

Records obtained from gage numbers EP 1 and EP 4 (see Fig. 25), both standard 1-Ω gages, are shown in Figs. 27 and 28. In both cases the pressure signal occurred during power supply turn on; the waveform shown is a difference signal between the test trace recorded prior to the event and the event signal. The gages were positioned prior to HE stacking and were referred to shot center; *i.e.*, the trigger probes, PZT piezoelectric ceramic elements, were placed ~3 inches in front of the gages on a sphere radius as shown in Fig. 24(a). Therefore, the early arrival of the shock wave at EP 1, with reference to its trigger probe, is not surprising. Similarly, it can be expected that the pressure profile would be rather unlike a plane wave in the vicinity of EP 1, and the shocks traveling perpendicular to the gage axis would distort the signal. The profile recorded by EP 4 indicates an initially lower pressure than expected (25 ± 10 kbar *vs.* 50 kbar) but a final pressure, before wire breaking, of 56 ± 10 kbar. The step increases may be due to multiple shocks from the various layers of HE. Shock arrival time, with reference to gage trigger probe, is very close to that expected, and the intermixing of event signal with power supply is caused by the unusually long turn-on signal associated with this single cable differential system.

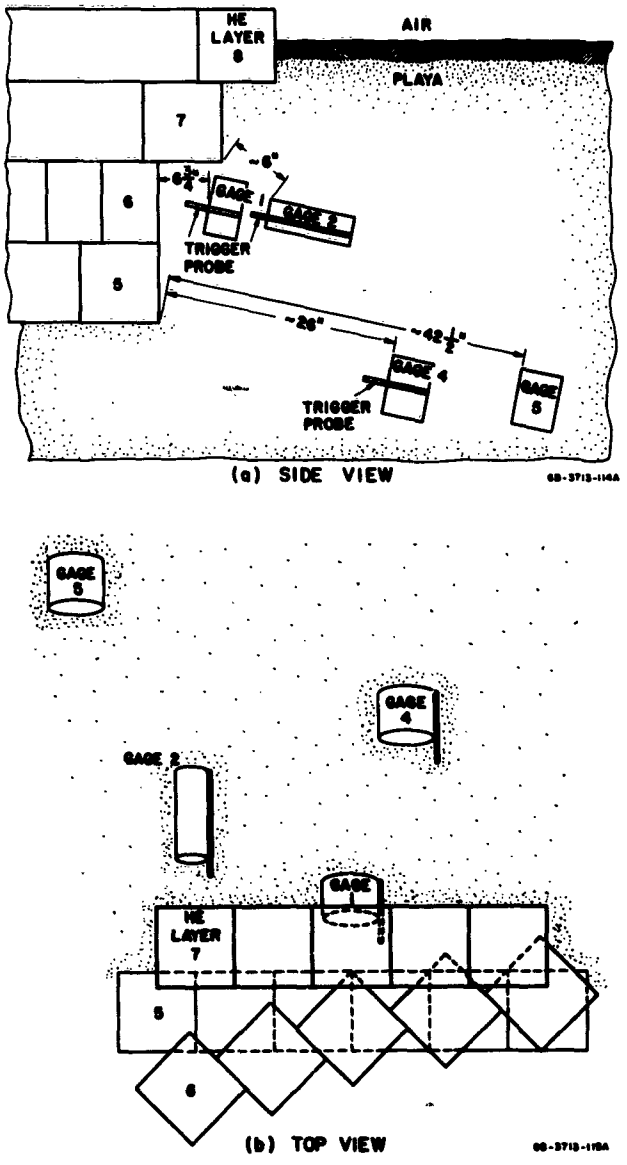

FIG. 24 GAGE PLACEMENT, FLAT TOP III

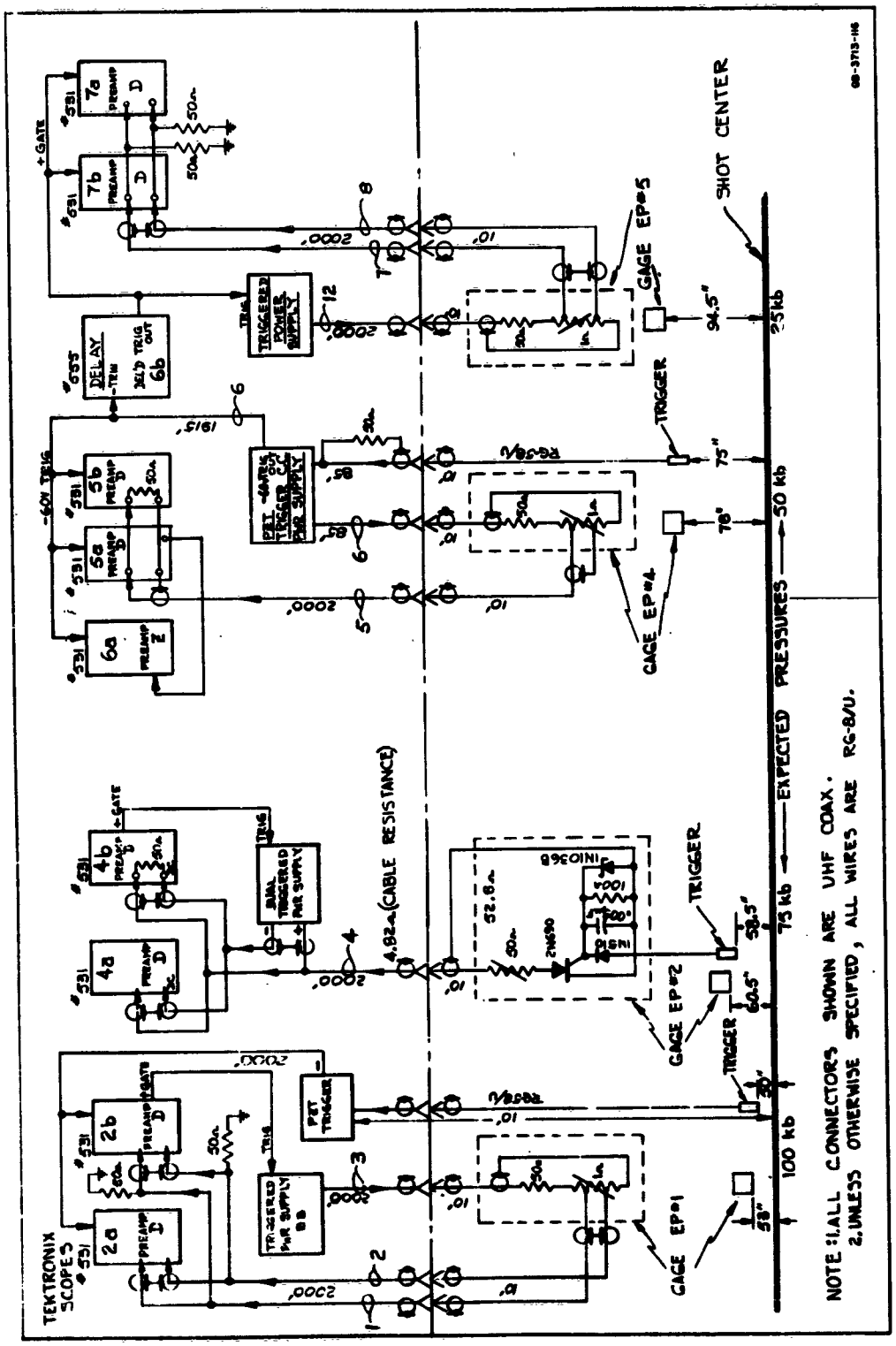

FIG. 25 RECORDING SCHEMATIC, FLAT TOP III

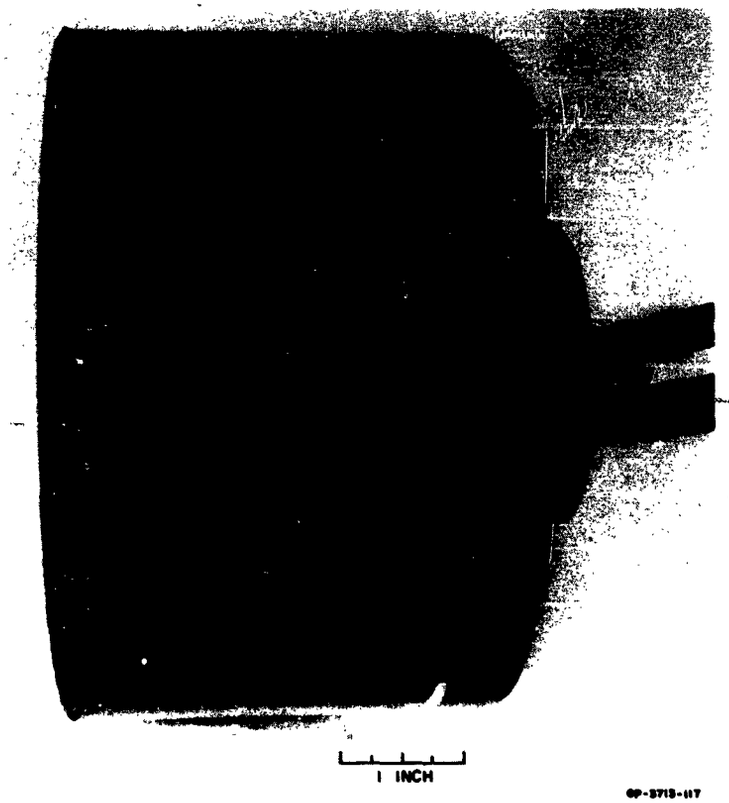

FIG. 26 1-Ω DIFFERENTIAL GAGE, FLAT TOP III

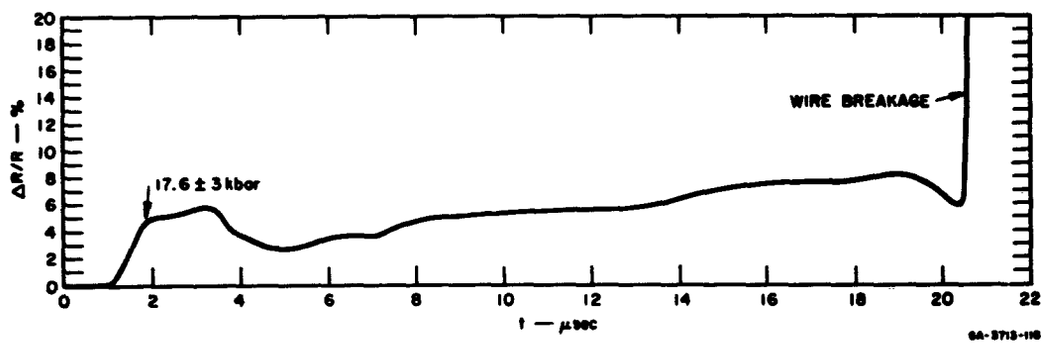

FIG. 27 1-Ω DIFFERENTIAL GAGE RECORD, EP1, FLAT TOP III

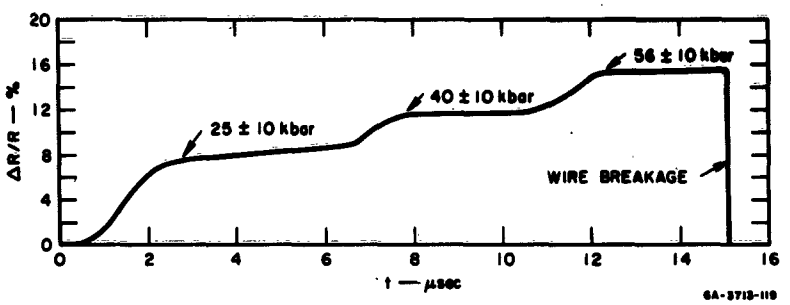

FIG. 28 1-Ω DIFFERENTIAL GAGE RECORD, EP4, FLAT TOP III

The 50-Ω gage (EP 2) records are off-scale on all oscilloscopes. It is not known whether this is trigger noise coupled from failure of the silicon controlled rectifier in the gage or an unusually large signal. In view of the pressure amplitudes recorded by EP 1 and EP 4, the former possibility is more likely. No oscilloscope traces were recorded from the last gage, EP 5. The reason for this is not known, but it is suspected that the delay oscilloscope (see Fig. 25) must have triggered prematurely since gage system EP 4, from which the trigger was derived, functioned satisfactorily.

4. Flat Top I

Four gages of the type shown in Fig. 26 were constructed for this event. Two were mounted on 8-inch diameter by ~18-inch-long marble cylinders which were placed in the limestone shot medium. One was placed in a column of grout and one on the HE stack. (Details are described in Reference 22.) Records were obtained from the latter two gage systems. Of the other two gages, one functioned satisfactorily except that the noise level at the time of recording masked the pressure record and one recording system appeared to have triggered early.

The record from the gage on the HE stack (reduced as in the preceding shots) is shown in Fig. 29. Both the duration, ~10 μsec, and the peak pressure, ~95 kbar, are lower than expected. One postshot test was conducted in which a gage of identical construction was subjected to a shock from a TNT explosive pad. The predicted peak pressure was 145 to 150 kbar, and a value of 147 kbar was recorded, the duration before stretching being as expected, ~20 μsec. Since the only major difference was that the laboratory gage was cemented to the TNT whereas the field gage was not, the coupling of gage to the TNT is suspect.

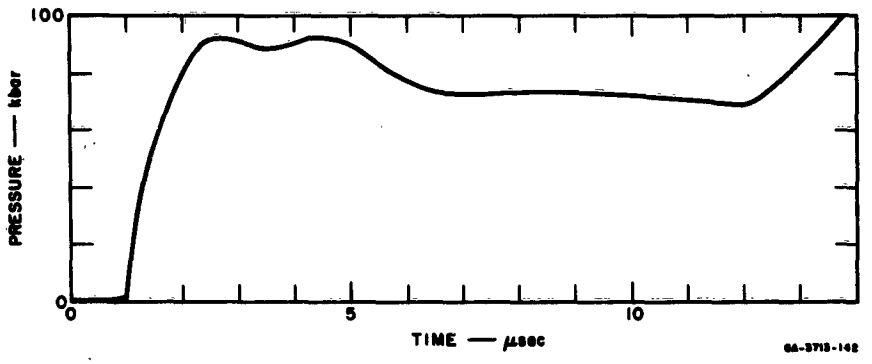

FIG. 29 1-Ω DIFFERENTIAL GAGE RECORD, HE STACK, FLAT TOP I

The grout gage record, again reduced, is shown in Fig. 30. The peak pressure reached is ~34 kbar and the duration at peak pressure is ~20 μsec. No further analysis has been made since the relation between the profile in grout and that in the surrounding limestone is not known.

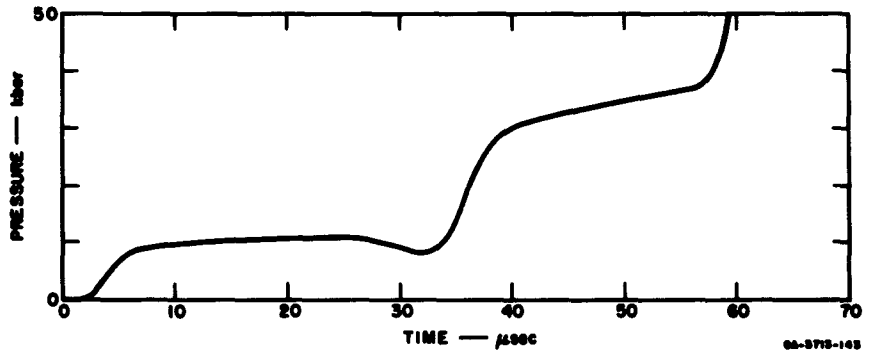

FIG. 30 1-Ω DIFFERENTIAL GAGE RECORD, GROUT COLUMN, FLAT TOP I

V CONCLUSIONS AND RECOMMENDATIONS

A. CONCLUSIONS

The general fidelity and response of a Manganin in C-7 epoxy transducer system appears suitable for use as a field test gage in a pressure range from as low as field recording limitations will permit, ~5 kbar, to at least 200 kbar gage pressure. Because C-7 is a material of low shock impedance when compared to most rocks, it can be used to measure pressure profiles of considerably higher rock pressures. The pressure limit in soils is approximately that of the gage since C-7 shock impedance is very similar to tuff, alluvium, and playa. In rocks where the gage and medium are mismatched, the pressure profile existing in the medium can be obtained if its equation of state is known. In the corresponding laboratory example chosen for analysis, C-7 epoxy on aluminum, the profile can be obtained, accurate to within ~10 percent, by a point for point impedance match solution; *i.e.*, the aluminum pressure can be obtained from the appropriate Hugoniots and cross curves.

The recording duration of the present type of gage, when used in media of dissimilar shock characteristics, is necessarily limited by gage dimensions. At moderate pressures, <100 kbar, and slowly decaying waves, laboratory tests have shown this to be ~20 μsec for a 6-inch diameter by 4-inch-thick gage. Long duration waves at higher pressures in the low impedance C-7 are beyond the test capability established by current laboratory explosive size limitations. Recording directly in higher impedance media may remove this test restriction. However, higher pressures will require either that there be a better match between the gage insulators and gage current-voltage leads or that the shock response of thin foils leads be better understood. This latter problem is a departure from the one-dimensional systems considered in the present work. However, such a two-dimensional study has important application to field test gage placement, *e.g.*, the behavior of a column of grout in a test medium of differing Hugoniot characteristics. If the profile in the medium can be obtained from measurements in the grout, the general gage placement is greatly simplified.

The feasibility of recording directly in other media has been demonstrated. However, the general response of Manganin in these media must be determined. In addition, a more universal wire configuration is required to permit recording in materials other than insulators.

Field test results are difficult to summarize since gage placement geometry differed considerably from the one-dimensional systems for which the gage was laboratory tested. Hence, little can be concluded from peak pressure measurements about gage functioning. Durations of recording, in most cases, were about those expected.

B. RECOMMENDATIONS

1. MANGANIN IN C-7 EPOXY

The Manganin in C-7 gage has been tested over part of the range of desired gage response characteristics and been found to perform satisfactorily. Since long duration recording at high pressures is a goal, it appears that response under these conditions must be either inferred from lower pressure work or measured in actual field tests. Although the overall response is satisfactory and is approaching a working tool for certain ranges of pressures and recording times, it is recommended that the limitations of the gage be determined by:

a) completing calculations of wire temperatures due to conduction of heat from the epoxy,

b) completing previously proposed work on lead-insulator matching and subsequent testing at high pressures, and

c) measuring hysteresis and duration of recording in a similar pressure range.

2. NEW GAGES

The most promising recent development is the direct measurement technique outlined in Section IV D. The eventual success of this method depends on continuing several areas of work:

a) developing methods of measuring pressure-time profiles with Manganin foils in conductors,

b) measuring Manganin response in various media for comparison with that obtained in C-7 and, in particular, measuring response to anisotropic stress.

3. Two-Dimensional Shock Studies

Concurrent with the above work, it is recommended that a program be initiated to investigate the behavior of materials under oblique, nonsteady state shocks by examining the relation between stress profiles in adjacent media of different equations of state. Although some theoretical work is possible, the emphasis would be on experimental work. The goals of this study should be 1) to predict gage component (lead) requirements and 2) to provide data useful in field installation of gages.

REFERENCES

1. Holzer, F., Measurements and Calculations of Peak Shock Wave Parameters from Underground Nuclear Detonations, UCRL-7805, 1964.

2. Eichelberger, R. J. and G. E. Hauver, "Solid State Transducers for Recording of Intense Pressure Pulses," *Les Ondes de Detonation*, Editions du Centre National de la Recherche Scientifique, 15 Quai Anatole-France, Paris (VII^{e}), 1961.

3. Jones, O. E., F. W. Nelson, and W. B. Benedick, "Dynamic Yield Behavior of Explosively Loaded Metals Determined by a Quartz Transducer Technique," J. Appl. Phys. 33, 3224-3232 (1962).

4. Keough, D. D., Pressure Transducer for Measuring Shock Wave Profiles, Final Report, Nov. 1, 1963, Contract No. DA-49-146-XZ-096, DASA 1414.

5. Bernstein, D., Pressure Transducer for Measuring Shock Profiles, Formal Report, June 15, 1962, DASA Contract No. DA-49-146-XZ-096.

6. Duvall, G. E., "Concepts of Shock Wave Propagation," Bull. Seismol. Soc. Am. 52, 869-893 (1962).

7. Doran, D. G., "Measurements of Shock Pressure in Solids," *High Pressure Measurement*, A. A. Giardini and E. C. Lloyd, (eds.), (Butterworth's, Washington, D.C.), 1963.

8. Semara, G. A. and A. A. Giardini, "High Pressure Manganin Gauges with Multiple Integral Calibrants," Rev. Sci. Instr. 35, 989-992 (1964).

9. Rice, M. H., R. G. McQueen, and J. M. Walsh, "Compression of Solids by Strong Shock Waves," *Solid State Physics*, D. Seitz and J. Turnbull (eds.), (Academic Press, N. Y.), 1958, Vol. 6.

10. Shapiro, A. H., *The Dynamics and Thermodynamics of Compressible Fluid Flow*, (Ronald Press, N.Y.), 1954, Vol. 2, Chaps. 24 and 25.

11. Fowles, G. R., Investigation of Equation of State of Porous Earth Media, WL-TDR-64-59, 1964.

12. Bernstein, D. and D. D. Keough, "Piezoresistivity of Manganin," J. Appl. Phys. 35, 1471-1474 (1964).

13. Lawson, A. W., "The Effect of Hydrostatic Pressure on the Electrical Resistivity of Metals," *Progress in Metal Physics*, (Pergamon Press, Ltd., London), 1963, pp. 1-43.

14. Strong, H. M., "Melting and Other Phase Transformations at High Pressures," *Progress in Very High Pressure Research*, F. P. Bundy, W. R. Hubbard, and H. M. Strong (eds.), (Wiley and Sons, Inc., N.Y.), 1961.

15. Bridgman, P. W., "Measurements of Certain Electrical Resistances, Compressibilities, and Thermal Expansion to 20,000 kg/cm3," Proc. Am. Acad. Arts and Sci. 70, 71-101 (1935).

16. Montgomery, P. W., H. Stromberg, G. H. Jura, and J. Jura, "Calibration of Bridgman Anvils, a Pressure Scale to 125 kbar," *High Pressure Measurement*, A. A. Giardini and E. C. Lloyd (eds.), (Butterworths, Washington, D.C.), 1963.

17. Lyakhov, G. M., "Shock Waves in Multicomponent Media," Akademyi Nauk SSSR. Otdelenie Tekhnicheskikh Nauk. Izvestia: Mekhanika i Mashinostroenic, 1959, No. 1.

18. Chabai, A. J., "Synthesis of Shock Hugoniots for Rock Materials," *Rock Mechanics*, C. Fairhurst, (ed.), (Pergamon Press, N.Y.), 1963.

19. Metallurgical Society Conferences, Vol. 9, *Response of Metals to High Velocity Deformations*, (Interscience Publishing Col., N. Y.), 1961.

20. Gregson, V. G., T. J. Ahrens, and C. F. Petersen, Dynamic Properties of Rocks. AFCRL-63-662. 1963.

21. Lombard, D., Hugoniot Equation of State of Rocks, Lawrence Radiation Laboratory, Report UCRL-6311, 1961.

22. Vincent, C., High Pressure Measurement in the Hydrodynamic Region, Final Report FLAT TOP, Project 1.3, Contract No. DA-49-146-XZ-207, 1964.

APPENDIX A

DETERMINATION OF TEST MATERIAL PRESSURE PROFILE FROM TRANSDUCER RECORD BY METHOD OF CHARACTERISTICS

By

DAVID K. CAMPBELL

APPENDIX A

DETERMINATION OF TEST MATERIAL PRESSURE PROFILE FROM TRANSDUCER RECORD BY METHOD OF CHARACTERISTICS

Consider the problem of an aluminum plate in contact with a slab of C-7 with a resistance wire gage imbedded in the C-7 two mm from the interface. At the back of the aluminum plate a shock is induced which passes through the aluminum and into the C-7. As the shock passes the gage, a pressure-time history is recorded. Reading values of pressure at arbitrary time intervals, 0.4 μsec, produces a series of pressure-time steps which can be used to generate the solution.

A working model of the transformation in the distance-time (x, t) plane is required. This depicts qualitatively what happens during the shock process, Fig. A-1 serving as the model.

The construction of the model is based on the simple qualitative attributes of shock waves, such as the production of both a reflected wave and a transmitted wave at the interface between materials of different impedances. From this, the model is constructed as follows:

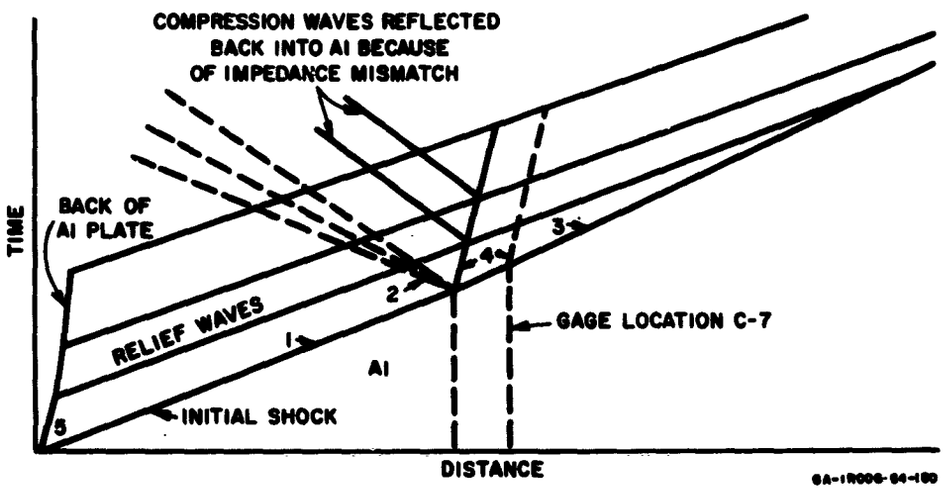

FIG. A-1 REFLECTION OF A DECAYING SHOCK AT ALUMINUM–EPOXY INTERFACE

The initial shock in the aluminum is drawn to the interface between the aluminum and the C-7. (The slope is arbitrary at this time. When the solution is actually being generated, it will depend on the pressure in the aluminum.) Since there is an impedance mismatch, there will be both reflected and transmitted waves. By using the method of impedance matching, it can be seen in Fig. A-2 that a shock is transmitted to the C-7 (line 3 in Fig. A-1) and a rarefaction is reflected into the aluminum. This rarefaction is depicted in Fig. A-1 in its usual form, *i.e.*, a rarefaction "fan" (lines 2).

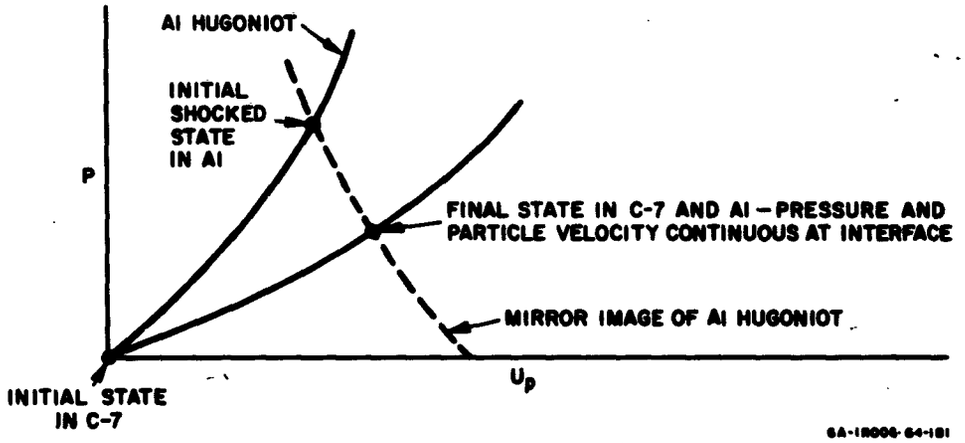

FIG. A-2 HUGONIOT AND CROSS CURVES IN THE PRESSURE–PARTICLE VELOCITY PLANE

When the shock initially stikes the back (see Fig. A-1) of the aluminum plate, this region of the plate accelerates to some nonzero particle velocity. Similarly, once the shock reaches the interface and the resistance wire, both assume some particle velocity. The wire velocity is assumed to be that of the moving mass of C-7, that is, the same as the interface velocity. The interface line (4), the line representing the back of the plate (5), and the relief waves originating at the back of the aluminum plate are shown schematically in Fig. A-1. In accordance with the theory of propagation of small pressure pulses, the slope of each of these right-traveling waves will be $dx/dt = (\bar{u} + \bar{c})$ where $\bar{u}$ and $\bar{c}$ are the average particle velocity and sound velocity in the two regions separated by the relief wave. If the relief waves were

left-traveling, their slope would be $dx/dt = \bar{u} - \bar{c}$. Note that when each relief wave reaches the interface, a compression is reflected into the aluminum and a relief wave is transmitted into the C-7. The number of relief waves drawn in the final solution is dependent on the number of pressure-time points that are read from the gage record.

The numerical solution can now be started. First, the portion of the model around the shock is enlarged, and each region (that is, each bounded area) is labeled (Fig. A-3).

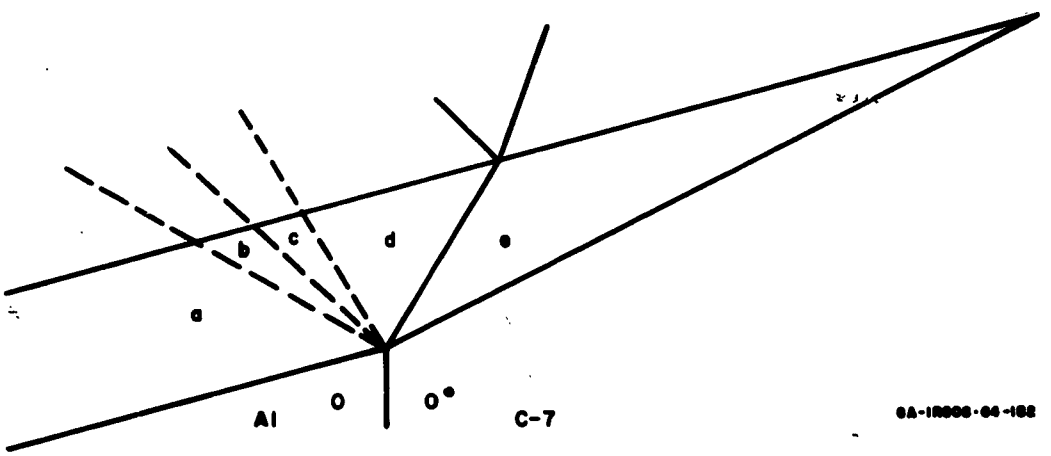

FIG. A-3 EXPANDED VIEW OF REGION 2, FIG. A-1

As an approximation, it is assumed that in each region the particle velocity and the sound velocity are constant throughout the region—the smaller the region, the more nearly correct this approximation. With this assumption, each *region* of the x,t plane will map into a single *point* on a plot of particle velocity *vs.* sound velocity. Thus the introduction of the particle velocity-sound velocity (u,c) plane becomes advantageous.

Without discussing the theory of characteristics, it can be shown[1] that for the Murnaghan equation of state (entropy assumed constant) $p = A[(\rho/\rho_0)^K - 1]$, the equations of the two families of curves that

[1] G. R. Fowles, "Attenuation of a Shock Wave Produced in a Solid by a Flying Plate" J. Appl. Phys. 31, 655-661 (1960)

represent characteristics in the u,c plane are

$$C^+ \text{ characteristics:} \quad \frac{dc}{du} = \frac{(K-1)}{2} \tag{A-1}$$

$$C^- \text{ characteristics:} \quad \frac{dc}{du} = -\frac{(K-1)}{2} \tag{A-2}$$

where K is the constant in the given Murnaghan equation Thus the characteristics are straight lines in the u,c plane.

In any single material, regions in the x,t plane which are separated only by left-traveling waves become points in the u,c plane which lie along common C^- characteristics; for instance, in Fig. A-3, regions a, b, c, and d lie along a common C^- characteristic (Fig. A-4).

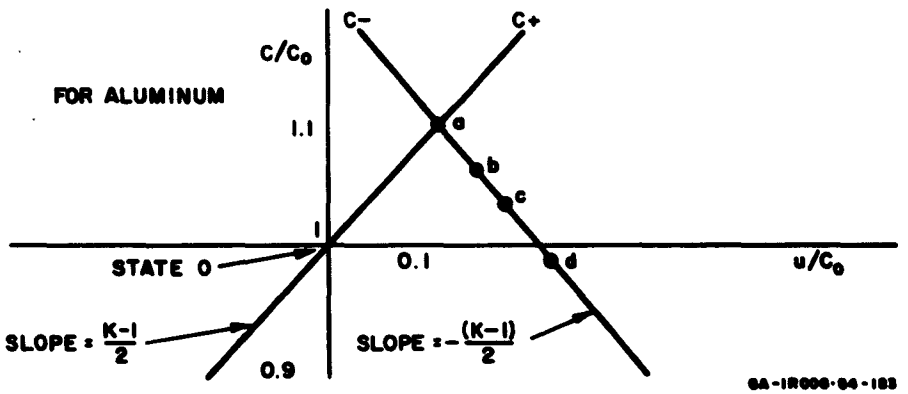

FIG. A-4 CHARACTERISTICS IN THE (NORMALIZED) SOUND VELOCITY–PARTICLE VELOCITY PLANE. It is common to plot c/c_0 vs. u/c_0 where c_0 is the sound velocity in a reference region labeled "O" in Figure 4.

Similarly, regions separated by only right-traveling waves lie along common C^+ characteristics. Using the approximation that the shock is an isentropic compression, regions O and a in Fig. A-3 are shown in Fig. A-4 lying on a common C^+ characteristic. Note that regions O and b, separated by both left- and right-traveling waves, do not lie on any common characteristic. It is clear that if u and c are known in region d, for example, and *either* u *or* c is known in regions a, b, and c, then all four points (a, b, c, d) can be located in the u,c plane, since they must lie along a common C^- characteristic. Once both sound velocity and particle

velocity are known at each of these points, the lines which represent the waves separating regions a and b, b and c, and c and d can be drawn. This is possible since, as mentioned previously, small pressure pulses propogate with velocities $dx/dt = \bar{u} + \bar{c}$ for right-traveling, $\bar{u} - \bar{c}$ for left-traveling waves.

Values of sound velocity, c, can be obtained as follows: There exists a one-to-one correspondence between sound velocity [defined by $c^2 = dp/d\rho$] and pressure under the assumption of constant entropy. In the case of a Murnaghan equation of state,

$$p = A[(\rho/\rho_0)^K - 1] \qquad \text{(A-3)}$$

and

$$c^2 = (AK/\rho_0)(\rho/\rho_0)^{K-1} = K(p + A)/\rho \quad . \qquad \text{(A-4)}$$

To clarify the above general discussion, the actual calculations for a specific problem will be partially reproduced. The pressure gage readings are shown in Fig. A-5. From the initial reading, the pressure in region e (Fig. A-3) of the C-7 is 148 kbar; using the Murnaghan equation of state for aluminum, this implies a particle velocity of 2.16 mm/μsec and a shock velocity of 6.09 mm/μsec in the C-7. Since particle velocity and pressure must be continuous across the interface, in region d of the aluminum, p = 148 kbar and u = 2.16 mm/μsec. After the shock in the

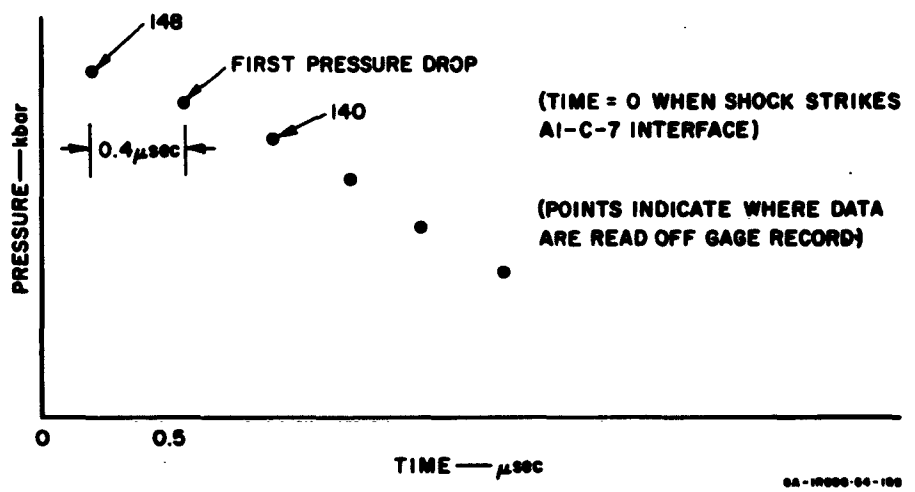

FIG. A-5 PRESSURE–TIME HISTORY AT WIRE

C-7 is drawn to proper slope (dx/dt = 6.09 mm/μsec) and the interface to its slope ($dx/dt = u_p$ = 2.16 mm/μsec), d is located in the u,c plane and the C- characteristic [slope = $-(K - 1)/2$] is drawn through it [Fig. A-6(a)]. Points a, b, and c in the u,c plane must lie on the characteristic through d. The location of point a in the u,c plane can be found by either (1) the

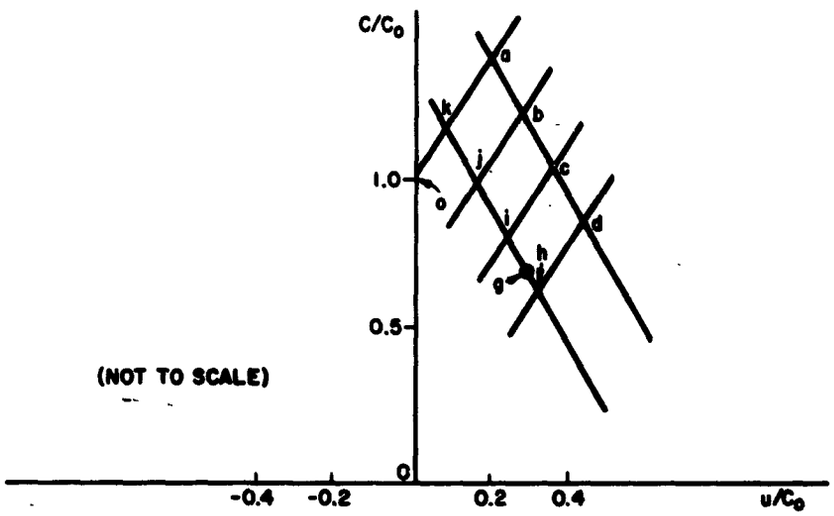

(a) SOUND SPEED, PARTICLE SPEED PLANE

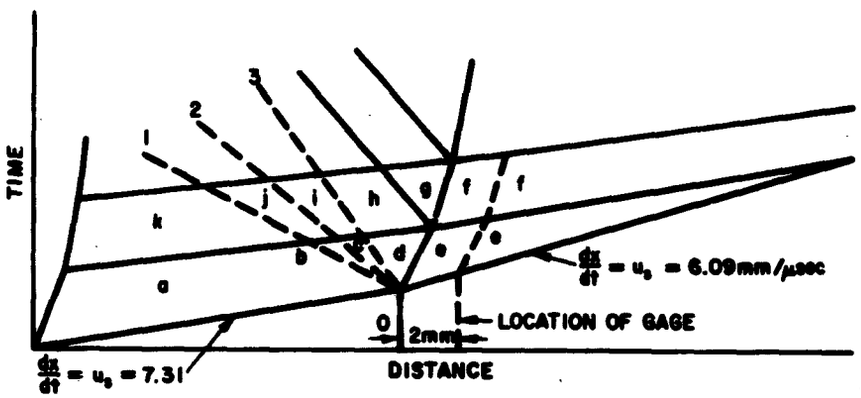

(b) TIME-DISTANCE PLANE

FIG. A-6 CHARACTERISTICS CURVES

impedance match method or (2) drawing the $C+$ characteristic through point O [slope $(K - 1)/2$] to intersect the $C-$ characteristic through d. The intersection must be point a, as was shown in the discussion of the model.

By using the impedance match procedure, the pressure in region a is 303 kbar. This corresponds to U_s = 7.31 mm/μsec and u_p = 1.48 mm/μsec. Since region a is assumed to extend to the back of the aluminum plate (to be discussed later), the velocity of the back of the aluminum plate is just u_p in region a, or dx/dt = 1.48 mm/μsec. Between regions a and d there is the rarefaction fan; the pressure drop across each of the elements of the fan is assumed equal, hence the pressures are p_a = 303 kbar, p_b = 252, p_c = 200, p_d = 148. Since sound speed is a unique function of pressure, this locates points b and c in the u,c plane. Thus the waves separating regions a, b, c, and d can be drawn with $dx/dt = u - c$ in each case. In Fig. A-6(b),

For wave (1), $dx/dt = \bar{u} - \bar{c} = -5.89$
For wave (2), $dx/dt = \bar{u} - \bar{c} = -5.34$
For wave (3), $dx/dt = \bar{u} - \bar{c} = -4.78$

This calculation completes the first "row" of regions in the aluminum. To begin the next row, containing regions g through k in Fig. A-6(b), the first pressure drop measured from the gage is determined. In this case the drop occurs 0.4 μsec after the initial shock reaches the wire. In Fig. A-6(b) the pressure in region f in the C-7 is 140 kbar (from gage record), which corresponds to a particle velocity of 2.08 mm/μsec. The wave is drawn with this slope through the point on the gage line 0.4 μsec above the point at which the initial shock reached the wire. Again, pressure and particle velocity must be continuous across the interface, so the location of point g in the u,c plane is known [Fig. A-6(a)]. Drawing the $C-$ characteristic through g in the u,c plane yields the line on which points h, i, j, and k must lie. But d and h are separated only by a right-traveling wave; hence they lie in a common $C+$ characteristic in the u,c plane. The intersection of the $C+$ characteristic through d and the $C-$ characteristic through g is h. Similarly, points i, j, and k are obtained by drawing the $C+$ characteristics through c, b, and a, respectively, until they intersect the $C-$ characteristic through g.

The lower particle velocity in f (as compared to e) indicates that the slopes of the interface and wire lines change; likewise the lower particle velocity in k (as compared to a) implies that the slope of the back of the aluminum plate changes.

The next "row" of regions is calculated in exactly the same manner. The state in C-7 is known from the gage record; this state defines the slope of the relief wave. The state in the aluminum at the interface is required to have the same pressure and particle velocity as the state in C-7 though the sound velocity is different This then locates the specific C- characteristic on which all points in the row lie; by extending the C+ characteristics through the points d and h, c and i, b and j, etc., all the points in the row are determined. The slopes of the waves in the x, t plane are then calculated as specified above. This procedure is continued until the data from the pressure gage record are exhausted. The values of the flow variables in each region are given in Table A-1.

Table A-1

FLOW PARAMETERS

Region	Pressure (kbar)	c (mm/μsec)	u_p (mm/μsec)
a	303	7.65	1.49
b	252	7.34	1.72
c	200	7.01	1.93
d	148	6.65	2.16
e	148	6.38	2.16
f	140	6.26	2.08
g	140	6.59	2.08
h	136	6.56	2.10
i	187	6.92	1.87
j	236	7.24	1.66
k	292	7.58	1.45

Reconstructing the undistorted wave in aluminum by this procedure necessarily limits the analysis to pressures equal to or less than the peak as recorded by the gage. This is because any relief waves which have intersected the initial shock before it reaches the gage must be neglected; they cannot be determined from the data available. Thus the pressure in region a of Fig. A-6, which was found to be 303 kbar, is almost certainly not the pressure at the back of the plate. As an example of this, consider the relief wave drawn as a dashed line in Fig. A-7; this

intersects the shock before it reaches the gage. The pressure in region z, which extends to the back of the aluminum plate, is greater than that in region a. But since there is no way by which the existence of z can be known from data at the gage, it must be assumed that region a extends to the back of the plate. Since the greater pressure in region z corresponds to a higher shock velocity than that in region a, the true profile of the shock will be altered; the shock including the effect of z is labeled "true shock" in Fig. A-7.

The results of the analysis are given in Sec. III-B.

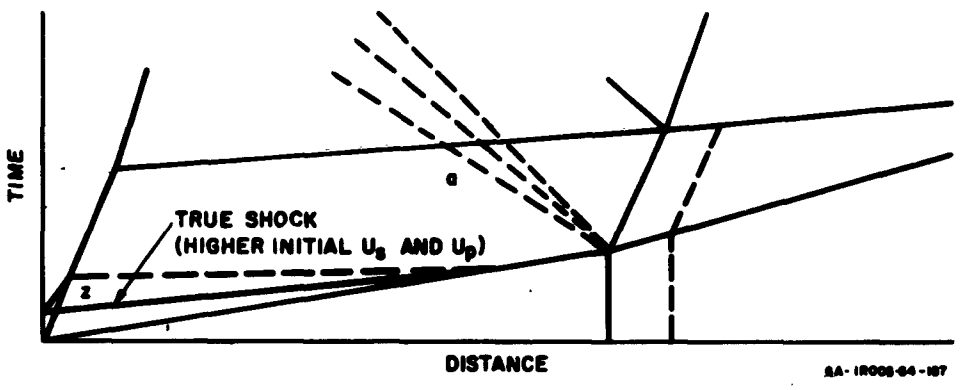

FIG. A-7 CHARACTERISTICS PATTERN FOR SHOCK WAVE DECAYING PRIOR TO REFLECTION AT ALUMINUM-EPOXY INTERFACE

APPENDIX B

HUGONIOT TEMPERATURE CALCULATIONS FOR C-7 EPOXY

By

P. H. MORAVEK

APPENDIX B

HUGONIOT TEMPERATURE CALCULATIONS FOR C-7 EPOXY

This appendix deals with calculations of shock temperatures reached in the C-7 insulator due to shock waves of amplitude greater than 500 kbar. The Hugoniot is represented by the equation[1]

$$P_H = 78.16\mu + 195.6\mu^2 + 221.4\mu^3 \text{ kbar} \qquad \text{(B-1)}$$

where

$$\mu = \left(\frac{V_{0H}}{V} - 1\right) \equiv \left(\frac{1}{v} - 1\right) . \qquad \text{(B-2)}$$

The symbols are defined below.

A. SYMBOLS AND CONSTANTS

1. Definitions of Symbols Used in Text

C_p	specific heat at constant pressure
C_{p0}	initial-value specific heat for C-7, cal/g°K
C'_{p0}	$4.186 \times 10^{-2} C_{p0}$, initial-value specific heat, kbar cm³/g° K
C_v	specific heat at constant volume
C_{vI}	specific heat in region I for $300^\circ K \leq T \leq 902°K$, kbar cm³/g°K
C_{vII}	specific heat in region II for $902°K \leq T$, kbar cm³/g°K
E_H	specific internal energy for Hugoniot states
E_K	specific internal energy for isentropes
$I_i^{(\alpha)}$	$(i = 1,2,3,4)(\alpha = A,B)$ integral expression depending on each Grüneisen ratio used
P	pressure, kbar
P_H	Hugoniot pressure, kbar
P_K	isentrope pressure, kbar
S	entropy, cal/g°K
T	temperature, °K

[1] John O. Erkman, private communication. Since Eq. (B-1) was fitted to data only up to about 100 kbar, we should be critical of results for high pressures.

T_{0H} initial temperature, °K

T_H temperature along the Hugoniot, °K

T_K temperature on isentrope, °K

V volume, cm^3/g

V_{0H} initial vol e at $P = 0$, cm^3/g

v $= V/V_{0H}$, relative volume parameter

α a constant in specific heat equation

β a constant in specific heat equation

Γ Grüneisen's ratio

Γ_{0H} initial value of Grüneisen's ratio for the data available on C-7

Γ'_{0H} initial value of Grüneisen's ratio for Lucite

$\Gamma_i^{(\alpha)}$ $(i = 1, 2, 3, 4)(\alpha = A, B)$ Grüneisen's ratio for the cases considered

μ $= \left(\frac{V_{0H}}{V} - 1\right)$, relative volume parameter

σ_2 upper probable error in measurement of Γ

σ_3 lower probable error in measurement of Γ

2. Values of Some Constants

C_{p0} = 0.387 cal/g°K at T_{0H}

C'_{p0} = 1.855×10^{-2} kbar $cm^3/g°K$

V_{VII} = 3.63×10^{-2} kbar $cm^3/g°K$ = 6.00 cal/atom°K based on average molecular weight 326.2 g/mole and average atomic weight 6.91 g/atom

T_{0H} = 300°K

V_{0H} = 0.8475 cm^3/g

σ_2 = 0.106

σ_3 = 0.352

Γ_{0H} = 0.790

Γ'_{0H} = 1.025

As reported previously,[2] approximate temperatures of the C-7 insulator were determined by calculations based on elastic and thermal data for Lucite along with certain simplifying assumptions such as: specific heat, C_V, is constant; Grüneisen's ratio,

$$\Gamma(V) = \frac{V}{C_V}\left(\frac{\partial P}{\partial T}\right)_V \qquad \text{(B-3)}$$

[1] P. H. Moravek, Appendix A, SRI Project GPU-3713, Progress Report No. 27, December 17, 1963.

is a constant; and Γ/V is constant for a second calculation. Lucite data for specific heat, compressibility, thermal expansion, density, and Hugonoit pressures were used because some of the properties are quite comparable to those of C-7, or at least were believed to be so; also, considerably more data were available for Lucite. There are, however, differences between C-7 and Lucite and a more accurate set of approximations is given in the present report to account for the C-7 Hugoniot data, the approximate variation of C-7 specific heat with temperature, and a range of straight-line approximations to Grüneisen's ratio as a function of volume based on experiment. The Grüneisen ratio for materials is really a function of both volume and temperature, but the temperature dependence is believed to be insignificant[3] except at low temperatures.

The previous approximate calculations were made for the shock-pressure range up to 125 kbar at which, using either Γ constant or Γ/V constant, the temperature becomes of the order of 10^3 °K. The results show the interesting fact that at 125 kbar the temperatures calculated for the two cases differ by less than seven percent.

B. PROCEDURE AND RESULTS

This appendix gives calculated Hugoniot temperatures for pressures exceeding 500 kbar for four slightly different Grüneisen's ratios.

1. Theory and Method

The present calculations of Hugoniot temperatures follow the previous method with less restrictive assumptions; only the principal differences will be discussed here.

We assume that the Hugoniot equation of state for C-7 epoxy given by Eq. (B-1) and that the Mie-Grüneisen equation of state

$$P_H - P_K = \frac{\Gamma}{V}(E_H - E_K) \quad , \tag{B-4}$$

which relates the Hugoniot data (subscript H) to isentrope data (subscript K) at a given volume V, is valid for this solid. The isentropes $P_K(V)$ are constructed by an iterative procedure from Hugoniot data as before. In

[3] J. M. Walsh and R. H. Christian, Phys. Rev. 97, 1544 (1955).

this case we have an experimental value at one point for Γ such that $\Gamma = 1.76\ ^{+6\%}_{-20\%}$ at $v = 0.63$. This value was measured by using the reflected shock wave technique[4] and assumes the solid obeys the Mie-Grüneisen equation of state. Also, since we have a value for Γ at initial conditions, determined from elastic and thermal data for Lucite, and another determined partly from C-7 data, we assume straight-line Γ equations as functions of relative volume between experimental and initial-conditions points (Region *A*). Two of these curves pass through the upper and lower limits of experimental probable error. Outside the range of the experimental points we assume Γ to be constant (Region *B*) at one of the three values, as shown in Fig. B-1. The equations of the four Γ curves and the range of their assumed validity are as follows:[5]

$$\left.\begin{aligned} \Gamma_1 &= \Gamma_{0H}(4.30 - 3.30v) \text{ for } 1.00 \geq v \geq 0.63; \\ \Gamma_1 &= 1.76 \text{ for } 0.63 \geq v \geq 0.49 \quad . \end{aligned}\right\} \quad \text{(B-5)}$$

$$\left.\begin{aligned} \Gamma_2 &= \Gamma_1(v) - \Gamma_{0H}\frac{\sigma_3}{0.292}(1 - v) \text{ for } 1.00 \geq v \geq 0.63; \\ \Gamma_2 &= 1.408 \text{ for } 0.63 \geq v \geq 0.49 \quad . \end{aligned}\right\} \quad \text{(B-6)}$$

$$\left.\begin{aligned} \Gamma_3 &= \Gamma_4(v) + \Gamma'_{0H}\frac{\sigma_2}{0.38}(1 - v) \text{ for } 1.00 \geq v \geq 0.63; \\ \Gamma_3 &= 1.866 \text{ for } 0.63 \geq v \geq 0.49 \quad . \end{aligned}\right\} \quad \text{(B-7)}$$

$$\left.\begin{aligned} \Gamma_4 &= \Gamma'_{0H}(2.94 - 1.94v) \text{ for } 1.00 \geq v \geq 0.63; \\ \Gamma_4 &= 1.76 \text{ for } 0.63 \geq v \geq 0.49 \quad . \end{aligned}\right\} \quad \text{(B-8)}$$

In each case the first equation is for Region *A* and the second is for Region *B*.

The results contain a set of isentropes, one for each Γ equation, and a set of curves of Hugoniot temperatures *vs.* pressure.

---

[4] See text, Section IV B for experimental technique and Appendix C for a calculation of Γ.

[5] The notation is to be taken so that $\Gamma_i(v)$ means "the ith gamma as a function of relative volume."

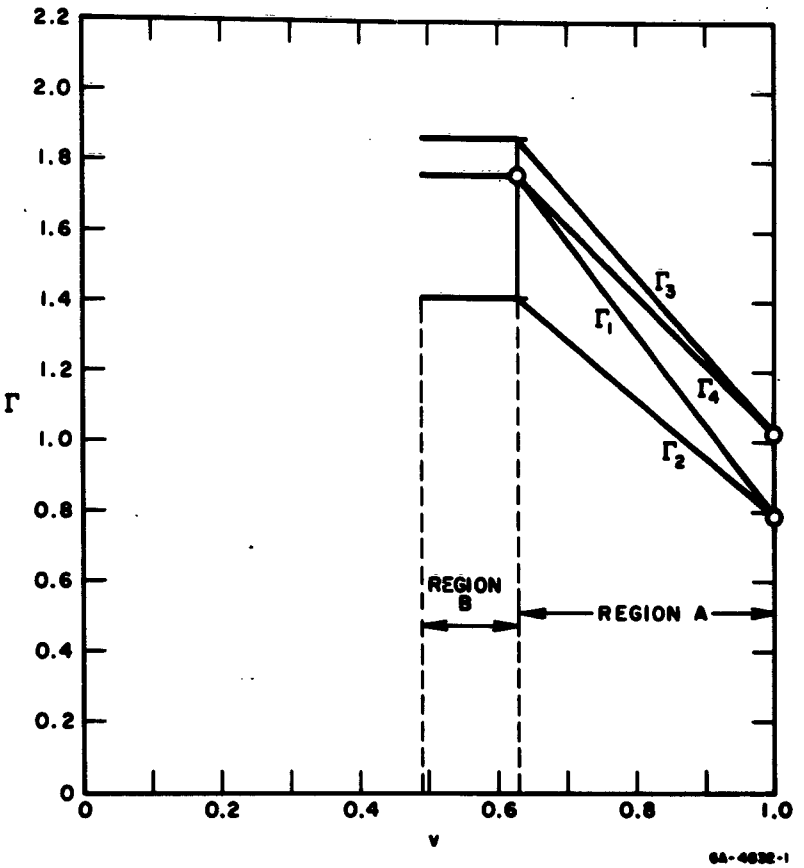

FIG. B-1 GRÜNEISEN'S RATIO IN TWO-REGIONS. Four Grüneisen's ratios used for regions A($1.0 \geq v \geq 0.63$) and B($0.63 \geq v \geq 0.49$). The spread in region A at $v = 1.0$ is due to the difference between initial data of Lucite (upper) and C-7 (lower). The spread in region B is due to the upper and lower limits of probable error of measurement.

In this calculation, the isentrope temperatures, T_K, are calculated according to the formula

$$\frac{T_K}{T_{0H}} = c^{-I_i}, \quad i = 1, 2, 3, 4 \quad . \tag{B-9}$$

The $I_i^{(\alpha)}$ are the integrals containing $\Gamma_i^{(\alpha)}$ and are given by

$$I_i^{(\alpha)}(v) = \int_1^v \frac{\Gamma_i^{(\alpha)}(v)dv}{v}, \quad i = 1, 2, 3, 4; \ \alpha = A, B \quad . \tag{B-10}$$

Explicitly, in the two regions A and B, where A corresponds to $1 \geq v \geq 0.63$ and B corresponds to $0.63 \geq v \geq 0.49$, the integrals can be shown to be[6]

$$\left.\begin{aligned} I_1^{(A)} &= \Gamma_{0H}(4.30\ \ln v - 3.30 + 3.30) \quad , \\ I_1^{(B)} &= I_1^{(A)}(0.63) + 1.76[\ln v - n(0.63)] \quad , \end{aligned}\right\} \tag{B-11}$$

$$\left.\begin{aligned} I_2^{(A)} &= I_1^{(A)}(v) - \frac{\Gamma_{0H}\sigma_3}{0.292}(\ln v - v + 1) \quad , \\ I_2^{(B)} &= I_2^{(A)}(0.63) + 1.408[\ln v - \ln(0.63)] \quad , \end{aligned}\right\} \tag{B-12}$$

$$\left.\begin{aligned} I_3^{(A)} &= I_4^{(A)}(v) + \frac{\Gamma'_{0H}\ \sigma_2}{0.38}(\ln v - v + 1) \quad , \\ I_3^{(B)} &= I_3^{(A)}(0.63) + 1.866[\ln v - \ln(0.63)] \quad , \end{aligned}\right\} \tag{B-13}$$

$$\left.\begin{aligned} I_4^{(A)} &= \Gamma'_{0H}(2.94\ \ln v - 1.94v + 1.94) \quad , \\ I_4^{(B)} &= I_4^{(A)}(0.63) + 1.866[nv - \ln(0.63)] \quad . \end{aligned}\right\} \tag{B-14}$$

In order to obtain the Hugoniot temperatures T_H from the isentrope temperatures T_K, we use specific heat data and integrate at constant volume for each value of v from the isentrope to the Hugoniot. That is, from the first law of thermodynamics

$$dE = TdS - PdV \tag{B-15}$$

and the identity

$$TdS = C_v\,dT + T\left(\frac{\partial P}{\partial T}\right)_v dV \quad , \tag{B-16}$$

[6] The functional notation of the previous footnote holds for $I_i^{(\alpha)}$ here. Also, $I_1^{(A)}(0.63)$ means "integral $I_1^{(A)}$ evaluated at $v = 0.63$."

we get (at constant volume)

$$dE = C_V\,dT \quad . \tag{B-17}$$

Integrating from isentrope to Hugoniot and substituting in the internal energy difference from Eq. (B-4) we get

$$\int_{T_K}^{T_H} C_V\,dT = E_H - E_K = \frac{V_{0H}}{\Gamma_i}\,v(P_H - P_K) \quad . \tag{B-18}$$

At this point we introduce specific heat as a function of temperature as shown in Fig. B-2. This curve is obtained partly from experiment and partly from theory as follows: We have a first-degree, least-squares fit of experimental data for specific heat at constant pressure which is good in the temperature range 323°K to 523°K, and is given by

$$C_p = C'_{p0}\,(\alpha + \beta T) \quad , \tag{B-19}$$

where $\alpha = 0.331$ and $\beta = 1.805 \times 10^{-3}/°K$. However, since we are dealing with temperatures considerably higher than this range, and since we lack experimental data at high temperatures, we assume the specific heat curve reaches the Dulong-Petit value of 6 cal/atom-degree for solids (which occurs at 902°K) and levels off at this value for the region of interest. This, of course, neglects possible electronic contribution at high temperatures. Further, since C_V does not differ greatly from C_p,[7] we define C_V in two regions to be (see Fig. B-2)

$$\text{Region } I\text{:}\quad C_{VI} \equiv C'_{P0}\,(\alpha + \beta T),\ 300°K \le T \le 902°K \quad , \tag{B-20}$$

$$\text{Region } II\text{:}\quad C_{VII} \equiv 3.63 \times 10^{-2}\ \text{kbar cm}^3/\text{g°K},\ 902°K \le T. \tag{B-21}$$

The value in (B-21) is just the Dulong-Petit value in the system of units we use here. Substituting these equations into the left-hand side of Eq. (B-18) we obtain equations for Hugoniot temperatures in the two regions:

[7] J. C. Slater, *Introduction to Chemical Physics*, McGraw-Hill, Inc., New York, 1939, p. 237.

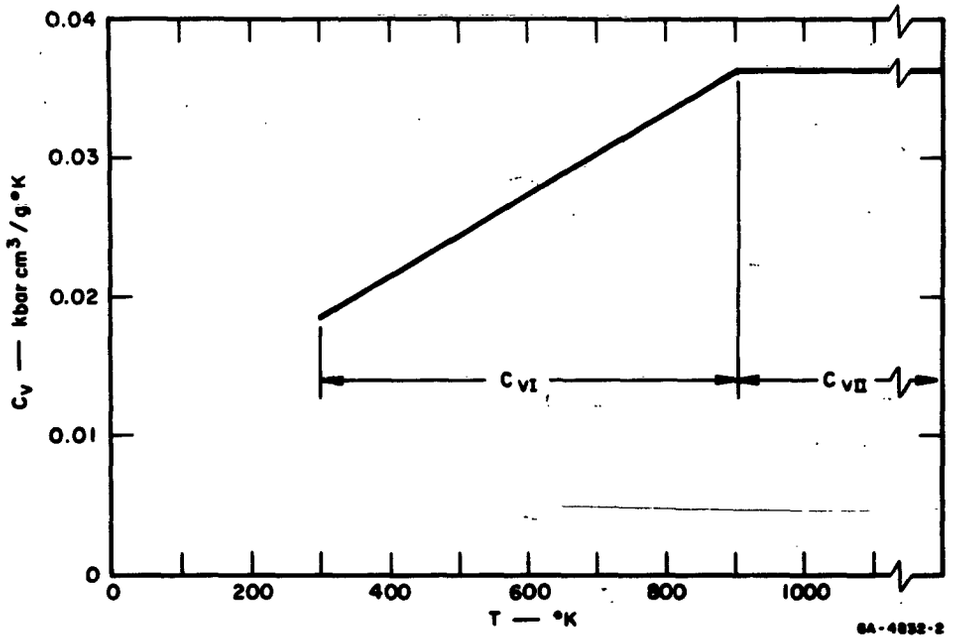

FIG. B-2 SPECIFIC HEAT IN TWO REGIONS. In region I($300 \leq T \leq 902$) C_{VI} is the first-degree fit of experimental data extrapolated to the Dulong-Petit value for C-7. In region II ($902 \leq T$) C_{VII} is taken to be constant at the Dulong-Petit value. The difference $C_P - C_V$ is neglected.

$$\text{Region } I: \quad T_H^2 + \frac{2\alpha}{\beta} T_H - \left[\frac{2}{\beta} \frac{V_{0H}}{C'_{P0}} \frac{v}{\Gamma_i} (P_H - P_K) + T_K^2 + \frac{2\alpha}{\beta} T_K \right] = 0 \quad . \tag{B-22}$$

$$\text{Region } II: \quad T_H = T_K + \frac{V_{0H}}{C_{VII}} \frac{v}{\Gamma_i} (P_H - P_K) \quad . \tag{B-23}$$

These are the equations that are solved for the Hugoniot temperatures for each Γ_i.

Some of the computational results are reproduced in graphic form in Fig. B-3 as a family of isentropes (one for each Γ used) along with the Hugoniot, Eq. (B-1), for comparison. The isentropes which develop a positive slope $dP_K/dv > 0$ clearly become nonphysical at very high pressures. This result is not inconsistent with the equation for the slope of the isentropes, which contains terms dependent upon Γ and dP_H/dv in such a way that a reduction in the magnitude of either or both of these quantities produces well-behaved isentropes. Furthermore, the fact that this

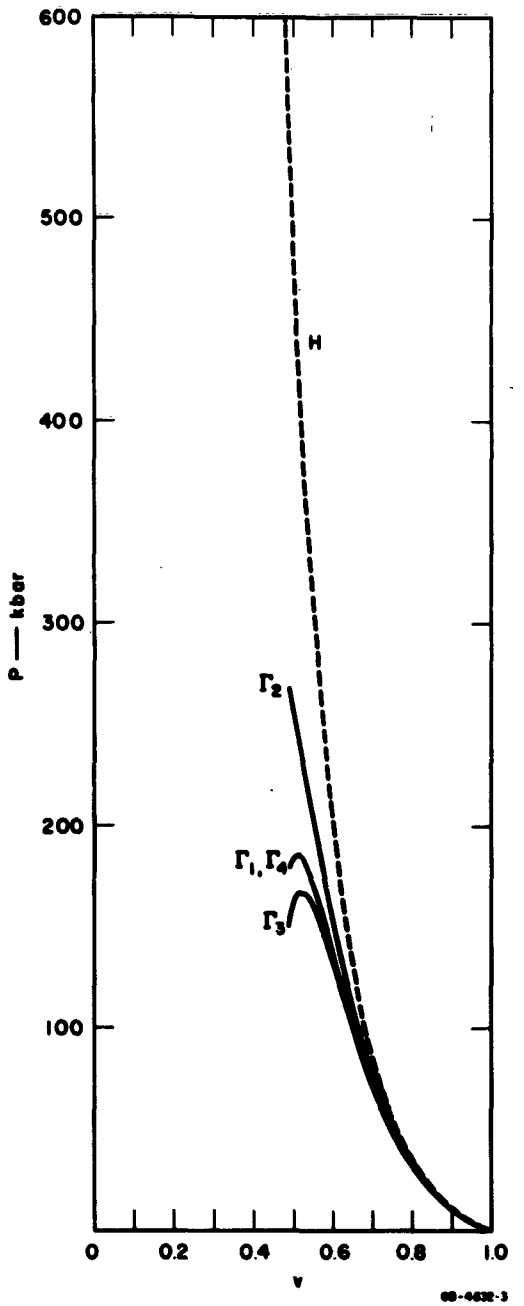

FIG. B-3 AUXILIARY COMPUTATIONAL RESULTS.
Comparison of isentropes of C-7 epoxy (labeled by the Γ used to generate each) and the Hugoniot (H). See text for explanation of the positive slopes.

occurs where we lack experimental data on Γ and P_H implies that the assumptions on Γ and the extrapolation of the P_H curve beyond the experimentally determined region may be invalid at very high pressures. Further investigation is needed in the high-pressure region. We note that the isentropes are quite sensitive to variations in Γ at high pressures.

Further intermediate results, the temperatures T_K along the isentropes, are given in Fig. B-4. They are labeled according to which Γ was used in their calculation.

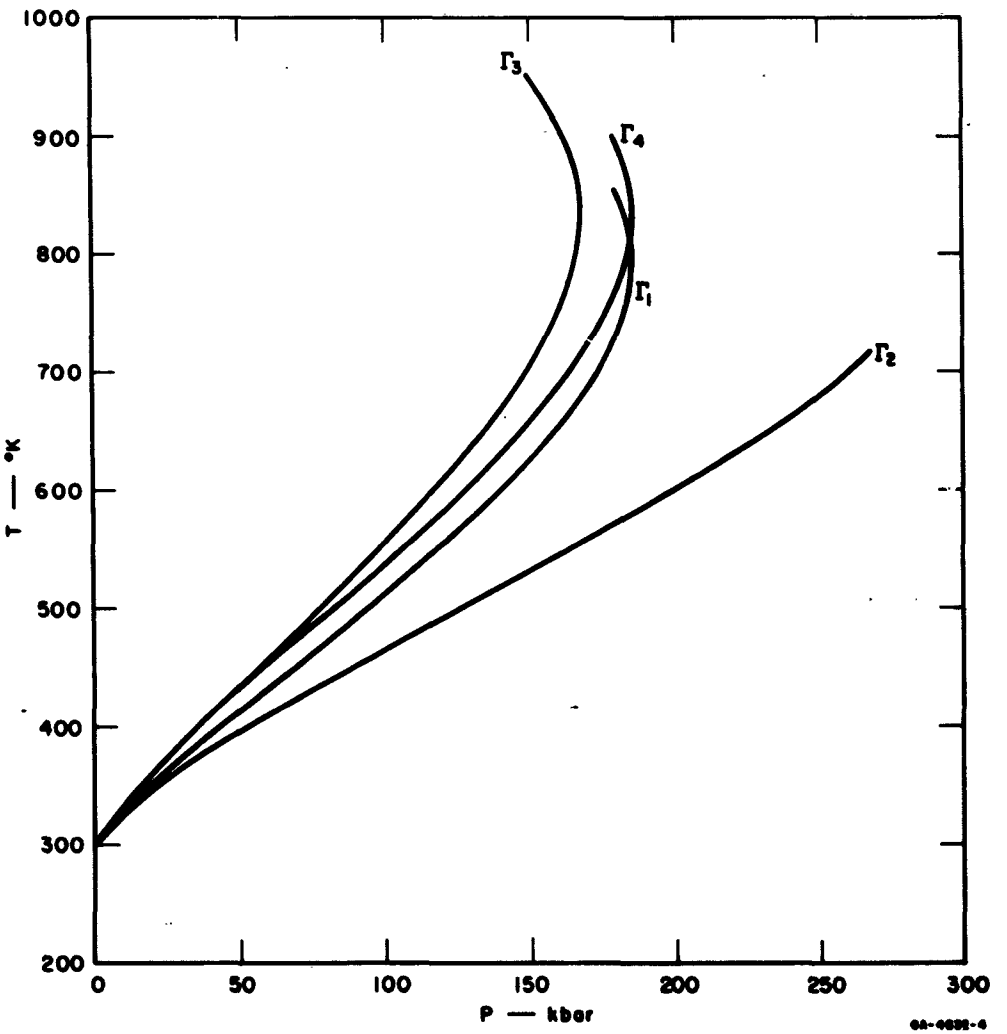

FIG. B-4 AUXILIARY COMPUTATIONAL RESULTS. Temperatures along the various isentropes of C-7 labeled by the Γ used in each calculation.

The principal results, the Hugoniot temperatures at very high pressures, are given in Fig. B-5. These Hugoniot temperature curves do not exhibit much sensitivity to variations in Γ as compared to that of the isentropes (Fig. B-3). From an examination of the isentropes (Fig. B-3) it appears that the best or most physically valid Γ used is Γ_2, which implies that the most reasonable Hugoniot-temperature curve is that labeled Γ_2 in Fig. B-5. The breaks in the curves of Fig. B-5 at approximately 900°K are a peculiarity of the computer program, which did not smoothly join regions *I* and *II* of the specific heat data.

Figure B-6 compares the present T_H calculations with the previous ones[2] made for Lucite up to 125 kbar. The present temperatures are seen to be somewhat lower than those calculated previously; this is in large part because of the higher values of specific heat used for the C-7.

2. P. H. Moravek, *ibid.*

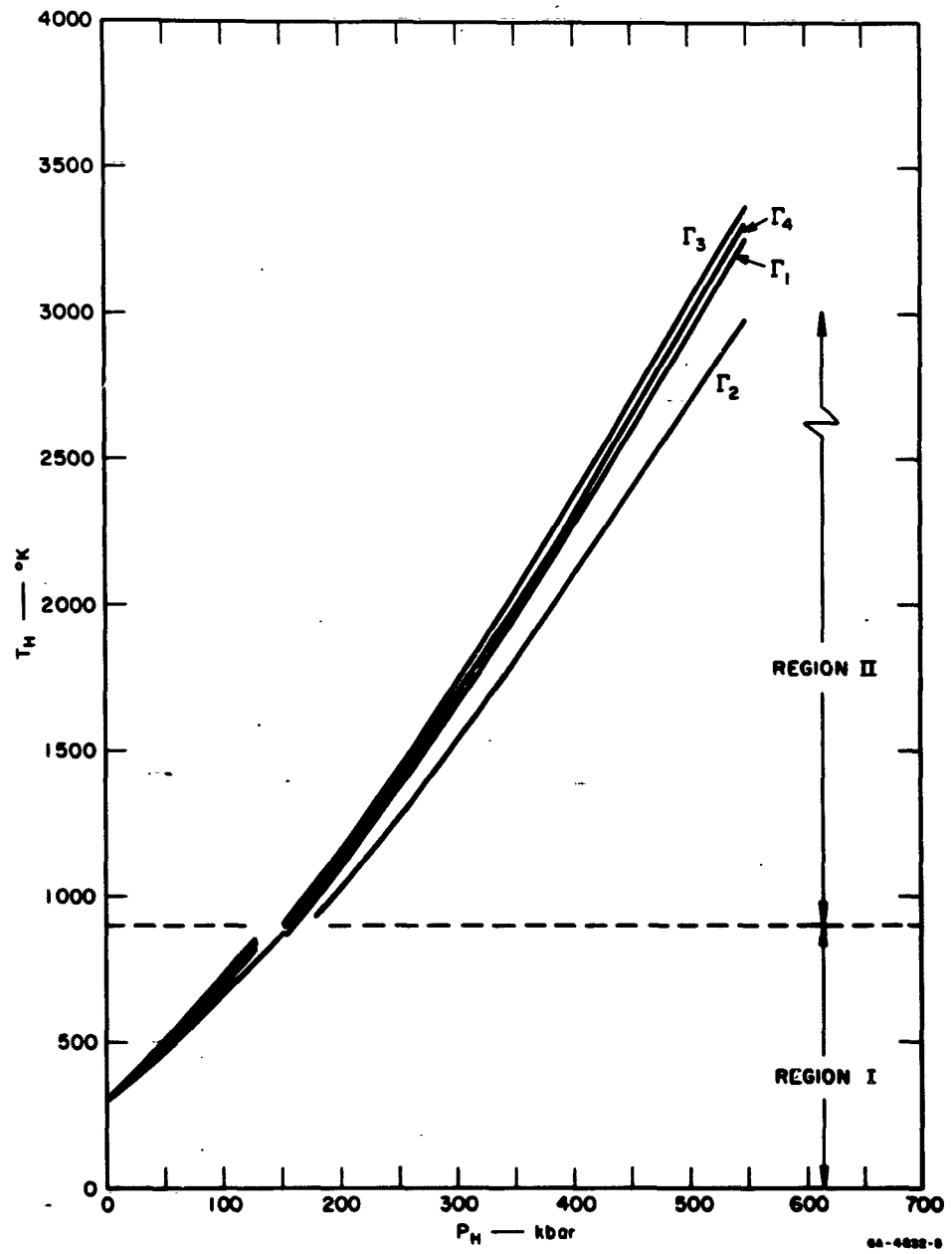

FIG. B-5 HUGONIOT TEMPERATURES OF C–7 EPOXY FOR FOUR DIFFERENT GRÜNEISEN'S RATIOS. Regions I and II are the temperature domains of the two different specific heat expressions. See Figs. B-1 and B-2.

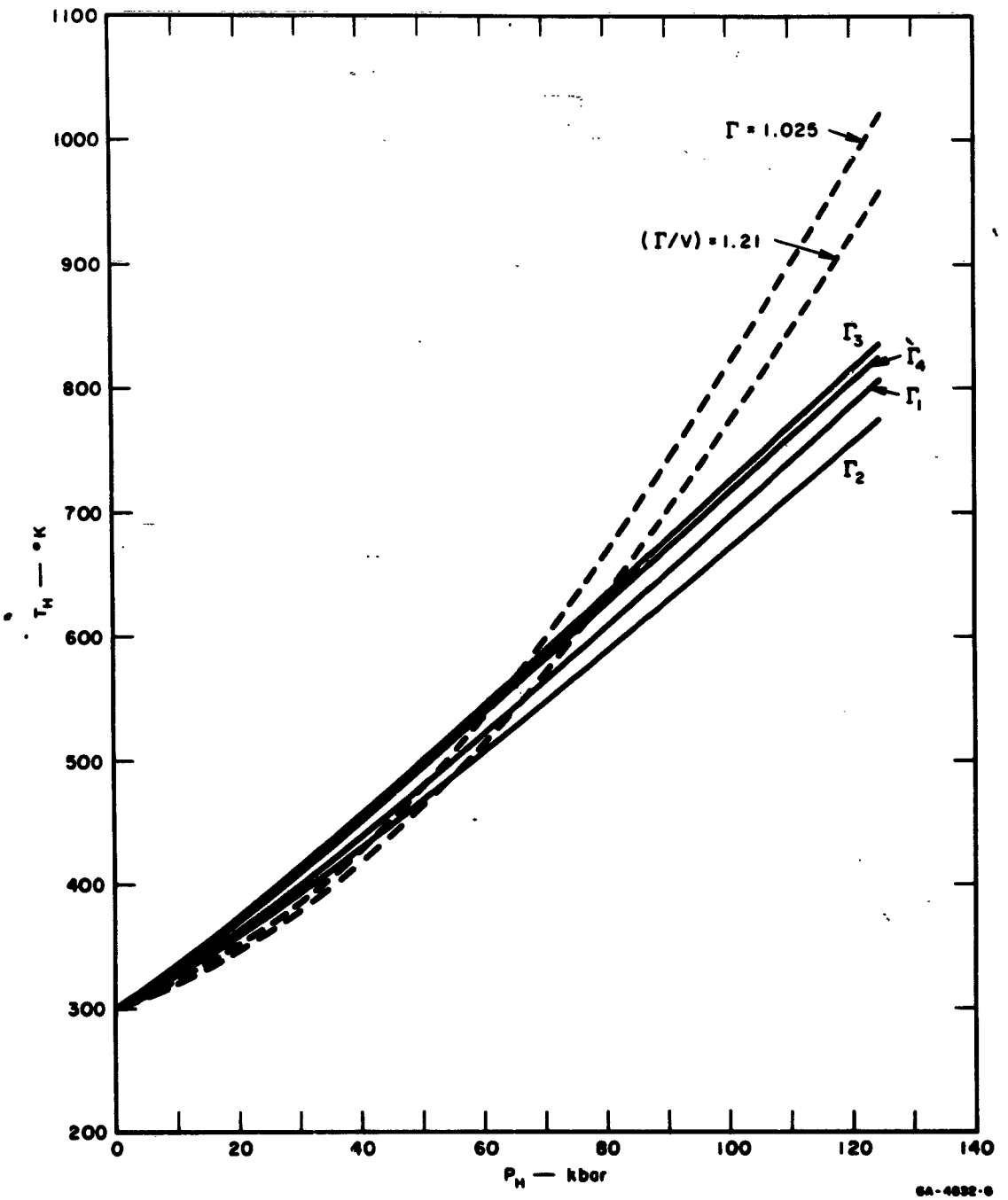

FIG. B-6 HUGONIOT TEMPERATURES, LOW PRESSURE REGION. Comparison of the present C-7 temperature calculations up to 125 kbar (solid curves) with those done previously with strictly Lucite data (dashed curves) assuming C_V constant.

APPENDIX C

CALCULATION OF GRÜNEISEN'S RATIO, Γ, FROM REFLECTED WAVE DATA

APPENDIX C

CALCULATION OF GRÜNEISEN'S RATIO, Γ, FROM REFLECTED WAVE DATA

The Grüneisen ratio, Γ, expresses the relation of pressure, P, to internal energy, E, of two states P_1E_1 and P_2E_2 at volume, V, of a thermodynamic system;[1]

$$P_1 - P_2 = \frac{\Gamma}{V}(E_1 - E_2) \qquad \text{(C-1)}$$

Thus, if a material is compressed to the volume, V, at two different Hugoniot states P_1VE_1 and P_2VE_2, Γ can be measured. The reflected wave shots (see Section IV of test) accomplish state P_2VE_2 by compressing C-7 from an initially-shocked state as shown in Fig. C-1. The state $P_1V_1E_1$ is reached by one shock from initial state $P_0V_0E_0$, whereas state $P_2V_2E_2(V_1 = V_2)$ is reached from shocked state $P_0'V_0'E_0'$; *i.e.*, the reflected wave Hugoniot is compared to the direct shock Hugoniot. The value of Γ is then determined from Eq. (C-1) as

$$\Gamma = V\frac{(P_1 - P_2)}{(E_1 - E_2)}$$

where

$$E_1 = E_0 + \frac{1}{2}P_1(V_0 - V_1)$$

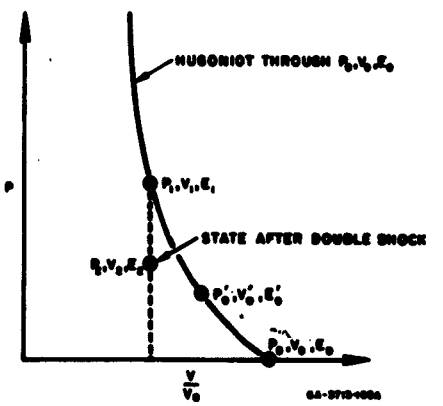

FIG. C-1 PRESSURE–VOLUME DIAGRAM OF C–7 STATES, REFLECTED WAVE SHOTS

1. M. H. Rice, R. G. McQueen, and J. M. Walsh, *Solid State Physics*, Vol. 6, F. Seitz and D. Turnbull, eds., Academic Press, N. Y., 1958, p. 40.

and

$$E_2 = E_0 + \frac{1}{2}(P_2 + P_0')(V_0' - V_2)$$

$$= E_0 + \frac{1}{2}P_0(V_0 - V_0') + \frac{1}{2}(P_2 + P_0')(V_0' - V_2)$$

Since

$$V_1 = V_2 = V,$$

$$\Gamma = V(P_1 - P_2)\left[\frac{1}{2}P_1(V_0 - V) - \frac{1}{2}P_0'(V_0 - V_0') - \frac{1}{2}(P_2 + P_0')(V_0' - V)\right]^{-1}$$

$$= \frac{2V}{V_0}(P_2 - P_2)\left[P_1\left(1 - \frac{V}{V_0}\right) - P_0'\left(1 - \frac{V_0'}{V_0}\right) - (P_2 + P_0')\left(\frac{V_0'}{V_0} - \frac{V}{V_0}\right)\right]^{-1} \quad \text{(C-2)}$$

The pressure and volume in state $P_0'V_0'E_0'$ are calculated from experimentally determined free surface velocities in the usual manner. The pressure in state ~~$P_2V_2E_2$ is assumed equal~~ to that in the reflecting plate which is calculated from measured plate shock velocity, free surface velocity, and initial density. The volume, $V_2 = 1/\rho_2$, is calculated from the Rankine-Hugoniot conservation equations which apply across the reflected shock front:[1]

$$\rho_0'(U_2 + u_0') = \rho_2(U_2 + u_2) \quad \text{(C-3)}$$

and

$$P_2 - P_0' = \rho_0'(U_2 + u_0')(u_0' - u_2) \quad \text{(C-4)}$$

where ρ_0', u_0' are the density and particle velocity, respectively, in state $P_0'V_0'E_0'$ and ρ_2, U_2, and u_2 are the density, shock velocity, and particle velocity, respectively, in state $P_2V_2E_2$. The density ρ_2 can be found by solving Eq. (C-4) for U_2 and substituting in Eq. (C-3).

A value of Γ can be calculated as outlined above from shot No. 9921 by first calculating the specific volume V_2 at pressure P_2 according to Eq. (C-3) and values of:

$$P_0' = 59 \text{ kbar}$$

$$V_0' = 0.63 \text{ cc}^3/\text{g}$$

$$u_0' = 1.14 \text{ mm}/\mu\text{sec}$$

$$P_2 = 145 \text{ kbar}$$

$$u_2 = 0.36 \text{ mm}/\mu\text{sec}$$

From Eq. (C-3):

$$U_2 = 3.73 \text{ mm}/\mu\text{sec}$$

which, upon substitution in Eq. (C-4), gives a specific density of

$$\rho_2 = \frac{1}{V_2} = 1.85 \text{ g/cc} \quad .$$

Since $V_1 = V_2$, a value of P_1 can be obtained from existing Hugoniot data.

Substitution in Eq. (C-2) then yields a value of $\Gamma = 1.76$ at $V/V_0 = 0.63$.

Official Use Only

Security Classification

DOCUMENT CONTROL DATA - R&D

(Security classification of title, body of abstract and indexing annotation must be entered when the overall report is classified)

1. ORIGINATING ACTIVITY *(Corporate author)* Stanford Research Institute 333 Ravenswood Avenue Menlo Park, California 94025	2a. REPORT SECURITY CLASSIFICATION Official Use Only 2b. GROUP

3. REPORT TITLE

Pressure Transducer for Measuring Shock Wave Profiles
Phase IX: Additional Gage Development

4. DESCRIPTIVE NOTES *(Type of report and inclusive dates)*

Final Report, November 1964

5. AUTHOR(S) *(Last name, first name, initial)*

Keough, Douglas D.

6. REPORT DATE	7a. TOTAL NO. OF PAGES	7b. NO. OF REFS
November 30, 1964	102	22

8a. CONTRACT OR GRANT NO.	9a. ORIGINATOR'S REPORT NUMBER(S)
DA-49-146-XZ-096	
b. PROJECT NO.	
c.	9b. OTHER REPORT NO(S) *(Any other numbers that may be assigned this report)*
d.	Final Report GSU-3713 (Phase IX)

10. AVAILABILITY/LIMITATION NOTICES

Qualified requesters may obtain copies of this report from DDC.
This report not authorized for open publication or distribution to Office of Technical Services, Department of Commerce.

11. SUPPLEMENTARY NOTES	12. SPONSORING MILITARY ACTIVITY
	Advanced Research Project Agency and Defense Atomic Support Agency

13. ABSTRACT

Peak pressure calibration, pressure-time profile response tests, and pressure-resistance hysteresis of the Manganin in C-7 epoxy transducer are described. It is shown that predicted and measured pressure-time profiles agree to within 10 percent. Also presented are: the transformation of profile measurements from transducer to test specimen, Hugoniot temperature calculations for C-7 epoxy up to ~500 kbar peak pressure, a method of constructing gages of Manganin in conducting materials, and gage field test results on the FLAT TOP series of events.

DD FORM 1 JAN 64 1473

Security Classification

14. KEY WORDS	LINK A		LINK B		LINK C	
	ROLE	WT	ROLE	WT	ROLE	WT

INSTRUCTIONS

1. **ORIGINATING ACTIVITY:** Enter the name and address of the contractor, subcontractor, grantee, Department of Defense activity or other organization *(corporate author)* issuing the report.

2a. **REPORT SECURITY CLASSIFICATION:** Enter the overall security classification of the report. Indicate whether "Restricted Data" is included. Marking is to be in accordance with appropriate security regulations.

2b. **GROUP:** Automatic downgrading is specified in DoD Directive 5200.10 and Armed Forces Industrial Manual. Enter the group number. Also, when applicable, show that optional markings have been used for Group 3 and Group 4 as authorized.

3. **REPORT TITLE:** Enter the complete report title in all capital letters. Titles in all cases should be unclassified. If a meaningful title cannot be selected without classification, show title classification in all capitals in parenthesis immediately following the title.

4. **DESCRIPTIVE NOTES:** If appropriate, enter the type of report, e.g., interim, progress, summary, annual, or final. Give the inclusive dates when a specific reporting period is covered.

5. **AUTHOR(S):** Enter the name(s) of author(s) as shown on or in the report. Enter last name, first name, middle initial. If military, show rank and branch of service. The name of the principal author is an absolute minimum requirement.

6. **REPORT DATE:** Enter the date of the report as day, month, year; or month, year. If more than one date appears on the report, use date of publication.

7a. **TOTAL NUMBER OF PAGES:** The total page count should follow normal pagination procedures, i.e., enter the number of pages containing information.

7b. **NUMBER OF REFERENCES:** Enter the total number of references cited in the report.

8a. **CONTRACT OR GRANT NUMBER:** If appropriate, enter the applicable number of the contract or grant under which the report was written.

8b, 8c, & 8d. **PROJECT NUMBER:** Enter the appropriate military department identification, such as project number, subproject number, system numbers, task number, etc.

9a. **ORIGINATOR'S REPORT NUMBER(S):** Enter the official report number by which the document will be identified and controlled by the originating activity. This number must be unique to this report.

9b. **OTHER REPORT NUMBER(S):** If the report has been assigned any other report numbers *(either by the originator or by the sponsor)*, also enter this number(s).

10. **AVAILABILITY/LIMITATION NOTICES:** Enter any limitations on further dissemination of the report, other than those imposed by security classification, using standard statements such as:

(1) "Qualified requesters may obtain copies of this report from DDC."

(2) "Foreign announcement and dissemination of this report by DDC is not authorized."

(3) "U. S. Government agencies may obtain copies of this report directly from DDC. Other qualified DDC users shall request through _____."

(4) "U. S. military agencies may obtain copies of this report directly from DDC. Other qualified users shall request through _____."

(5) "All distribution of this report is controlled. Qualified DDC users shall request through _____."

If the report has been furnished to the Office of Technical Services, Department of Commerce, for sale to the public, indicate this fact and enter the price, if known.

11. **SUPPLEMENTARY NOTES:** Use for additional explanatory notes.

12. **SPONSORING MILITARY ACTIVITY:** Enter the name of the departmental project office or laboratory sponsoring *(paying for)* the research and development. Include address.

13. **ABSTRACT:** Enter an abstract giving a brief and factual summary of the document indicative of the report, even though it may also appear elsewhere in the body of the technical report. If additional space is required, a continuation sheet shall be attached.

It is highly desirable that the abstract of classified reports be unclassified. Each paragraph of the abstract shall end with an indication of the military security classification of the information in the paragraph, represented as *(TS)*, *(S)*, *(C)*, or *(U)*.

There is no limitation on the length of the abstract. However, the suggested length is from 150 to 225 words.

14. **KEY WORDS:** Key words are technically meaningful terms or short phrases that characterize a report and may be used as index entries for cataloging the report. Key words must be selected so that no security classification is required. Identifiers, such as equipment model designation, trade name, military project code name, geographic location, may be used as key words but will be followed by an indication of technical context. The assignment of links, roles, and weights is optional.

DD FORM 1 JAN 64 1473 (BACK)